RTD-TDR-63-4001

STUDY TO INVESTIGATE AND DEMONSTRATE FEASIBILITY OF A NUCLEAR GYRO

TECHNICAL DOCUMENTARY REPORT No. RTD-TDR-63-4001

NOVEMBER, 1963

AF Avionics Laboratory
Research and Technology Division
Air Force Systems Command
Wright-Patterson Air Force Base, Ohio

Project No. 4431 Task No. 443111

(Prepared under Contract No. AF33(657)8804
by Arma Divison, American Bosch Arma Corporation,
Garden City, New York
Author: Dr. C. D. Bock)

STUDY TO INVESTIGATE AND DEMONSTRATE FEASIBILITY OF A NUCLEAR GYRO

TECHNICAL DOCUMENTARY REPORT No. RTD-TDR-63-4001

NOVEMBER, 1963

AF Avionics Laboratory
Research and Technology Division
Air Force Systems Command
Wright-Patterson Air Force Base, Ohio

Project No. 4431 Task No. 443111

(Prepared under Contract No. AF33(657)8804
by Arma Divison, American Bosch Arma Corporation,
Garden City, New York
Author: Dr. C. D. Bock)

NOTICES

When Government drawings, specifications, or other data are used for any purpose other than in connection with a definitely related Government procurement operation, the United States Government thereby incurs no responsibility nor any obligation whatsoever; and the fact that the Government may have formulated, furnished, or in any way supplied the said drawings, specifications, or other data, is not to be regarded by implication or otherwise as in any manner licensing the holder or any other person or corporation, or conveying any rights or permission to manufacture, use, or sell any patented invention that may in any way be related thereto.

Qualified requesters may obtain copies of this report from the Defense Documentation Center (DDC), (formerly ASTIA), Cameron Station, Bldg. 5, 5010 Duke Street, Alexandria 4, Virginia.

This report has been released to the Office of Technical Services, U.S. Department of Commerce, Washington 25, D.C., for sale to the general public.

Copies of this report should not be returned to the Aeronautical Systems Division unless return is required by security considerations, contractual obligations, or notice on a specific document.

FORWARD

This report was prepared by Arma Division, American Bosch Arma Corp. on Air Force Contract AF33(657)8804, under Task No. 443111 of Project No. 4431, "Study to Investigate and Demonstrate the Feasibility of a Nuclear Gyro". The work was administered under the direction of AF Avionics Laboratory, Research and Technology Division, Air Force Systems Command. Captain S. L. Bachman was project engineer for the Laboratory.

The studies presented began in July, 1962, and represent the effort of the Research Department of Arma Division. H. Levenstein was the engineer for research activity for Arma Division.

Although the studies were a group effort, the chief contributors and their fields of interest were: Dr. B. Zarwyn; Dr. C. D. Bock, theory; Dr. A. Eberstein, materials; G. Davidson,electronics; M. Taraswich, cryogenies; and N. Altmayer, mathematical analysis.

The cooperation of Prof. C. D. Jeffries of the University of California, Berkeley, California is gratefully acknowledged. The Arma Division is especially grateful for the analysis of enhancement in solids and liquids contributed by Prof. Jeffries and for his permission to reproduce his results.

This report is the final report and it concludes the work on Contract AF33(657)8804. The Contractor's report number is DS-63-R531-55.

This report is unclassified.

ABSTRACT

An investigation into the applicability of solids in a nuclear gyroscope was made. The performance of rate and position gyroscopes was evaluated using experimentally determined characteristics of representative types of solids and some liquids, and a breadboard pulsed coil position gyro was fabricated to test principles and to provide direct experimental data on materials. It was concluded that normal solids would not admit inertial quality performance. However one exception was found. It was further noted that liquids categorically allow performance superior to solids.

TABLE OF CONTENTS

TABLE OF CONTENTS (Continued)

LIST OF TABLES

LIST OF ILLUSTRATIONS

1. INTRODUCTION

The analogy between the spinning elements of the nucleus and the gyroscope wheel has prompted investigators for many years to seek instrumentation which would use this spin as the space reference in a non-mechanical gyroscope or inertial stabilization system. Designs of nuclear gyroscopes are based on the nuclear paramagnetic property of some materials and the application of nuclear magnetic resonance techniques. A major consideration in all the designs has been the problem of the type of material to use and its environmental conditions to give optimum gyro performance.

In a general way non-solid materials have been reasonably well explored although fundamental research continued to bring new characteristics to light, particularly with respect to changes in the physical environment of temperature and pressure. The capabilities of solids are not nearly as well understood. Accordingly a program to study the feasibility of a solid state nuclear gyro was undertaken. The results of this study are reported in this report.

The performance objectives against which the potential gyro is to be measured is a drift rate of 0.001 degrees per hour, a figure somewhat better than the fixed drift (uncompensatable) of the best current inertial systems. Other desirable features are ruggedness, reliability, and non-mechanical operation.

The approach was both analytical and experimental. On the analytical side a search was made of the literature on nuclear magnetic resonance in solids, theoretical descriptions of system performance were developed, and various solids were tested in these equations. Techniques of performance improvement were examined for applicability, including microwave and optical enhancement possibilities, and the ramifications of doped solids were explored for a guide to potentially useful materials.

On the experimental side a breadboard model of a two-degree of freedom position gyro was fabricated; it offered a means for directly examining the gyroscopic utility of materials and was of interest intrinsically due to its novelty. Further it offered direct experimental confirmation of performance theories arising from material properties. The expressions for signal-to-noise ratio and drift due to magnetization noise were developed for this system.

Finally, with the present program completed, conclusions can be made regarding the feasibility of a solid-state nuclear gyro. The conclusions are based on the evaluation of nuclear gyro performance for solids; comparison with a liquid-state nuclear gyro indicates the liquid phase is preferable for high gyro performance.

2. NUCLEAR GYRO PERFORMANCE EQUATIONS

The applicability of solids in a nuclear magnetic resonance gyro was investigated analytically. This investigation proceeded along two lines. A complete review of the literature, classified and unclassified, was made pertaining to nmr studies performed with solids. Proposals and presentations describing the performance of a gyroscope based on the gyroscope properties of a collection of nuclear spins were reviewed. The literature review will be discussed in the next section. In this section the formulae which have been developed and used to evaluate nuclear gyro performance will be presented.

2.1. BACKGROUND

It is not possible to develop the equations showing resonance error measurements and directional drift for a generalized nmr gyro. This is especially true for solids. Even in ordinary nmr of solids, a complete analysis of the magnetization, relaxation times and signal have never been worked out. Consequently it is necessary to analyze the performance of various classes of gyros and then evaluate each system as a function of different solids.

We will analyze and discuss two classes of gyros, the rate gyro and the position gyro. Our review indicated that only two rate gyro schemes have been sufficiently detailed to be considered for our evaluation of solids, the one proposed by GPI (Ref. 1) in their March 1960 report and the one by Motorola, Inc. (Ref. 2) of April, 1962. For the position gyro we will use the scheme and formulae developed by Arma and discussed in detail in section 6. This represents the only position gyro analysis ever completed since no other was uncovered in the literature.

Both rate gyro approaches are based on the principle that the resonant frequency of the rf oscillator of the nmr system is a linear function of the inertial rate of the nmr apparatus. This effect results from the inertial rotation of the driving field coils about the polarizing field direction.

It will be assumed from the start that Bloch's equations can be used for describing the magnetization of solids within certain limits. Redfield (Ref. 3) has stated that the Bloch equations may be considered an approximation for describing behavior in a solid under certain limited conditions. As we stated before, due to the complexity of the problem and to arrive at some evaluation of the performance of solids in the nuclear gyro the derived equations for drift and signal-to-noise ratio will be applied here.

2.2. RATE GYRO PERFORMANCE EQUATIONS - SYSTEM I

The Motorola analysis of nuclear gyro performance assumes a conventional nmr scheme with a nuclear spin system that is described by the

Bloch equations. The sample is contained within a coil of a shunt resonant circuit which detects an rf signal whose amplitude is proportional to the nuclear magnetization component Mu (the component of M parallel to H_1 in the rotating frame). That is,

$$S = C\,Mu \tag{1}$$

where C is a constant.

Any instrumentation noise An accompanying the signal S constitutes an error and will cause a directional drift in the nuclear gyro. The mean square directional drift for a sample of spin-lattice relaxation T_1 and spin-spin relaxation time T_2 is given by

$$E\left[D^2_{M_u}(N)\right] = \frac{tT_c\,(1+R)^2}{8RT_2^2}\left(\frac{N}{\eta S}\right)^2 \tag{2}$$

where
- t = drift time interval
- T_c = period of cutoff frequency of signal output circuit
- $R = \gamma^2 H_1^2 T_1 T_2$
- η = enhancement factor

and S/N is the peak signal to rms noise ratio which was developed by Bloembergen, Purcell and Pound (Ref. 4) and is expressed by

$$S/N = 1.6 \times 10^{-4}\,\frac{Nh^2\gamma^{11/4}H^{7/4}I(I+1)}{V_c^{1/3}k^{3/2}T^{3/2}}\left(\frac{T_2}{BFT_1}\right)^{1/2} \tag{3}$$

where
- V_c = volume of coil
- N = total number of nuclei in the spin system
- I = nuclear spin
- T = ambient temperature
- H = polarizing field
- h, k = constants
- γ = gyromagnetic ratio of sample
- B = signal bandwidth
- F = noise figure

Another source of error which contributes to the gyro directional drift is that due to the magnetization noise in the nuclear spin system; this noise is an inherent property of the nuclear spin system so that its corresponding error and drift are independent of the type of instrumentation used to observe the signal. It is estimated that the rms nuclear magnetization noise is of the order $\mu N^{1/2}/V$ in a bandwidth of the order of $1/Z_0T$ where μ is the nuclear

magnetic moment, V is the sample volume, and Z_0 is the resonance saturation factor (1/1+R). This noise will give rise to a directional drift

$$E\left[D_M^2(M)\right] = \frac{2t(1+R)T_1^2}{NRT_2^3}\left(\frac{3IkT}{\mu(I+1)H}\right)^2 \qquad (4)$$

This equation represents the minimum possible drift for any type of signal and for a nuclear spin system obeying the Bloch steady state magnetization equations.

2.3. RATE GYRO PERFORMANCE EQUATIONS - SYSTEM II

The approach presented by the GPI group is basically similar to that of the Motorola group. A conventional nmr system is assumed with a spin system that may be represented by the Bloch equations. This scheme deviates from the Motorola presentation in that the signal or voltage induced in the pick-up coil is related to the time derivative of the component of the magnetization: that is,

$$S = KM_y \qquad \text{where} \qquad M_y = A\sin Wt + B\cos wt \qquad (5)$$

where K is a constant.

Any instrument noise will cause a shift in the mean frequency ($W = \gamma H$) which will lead to an uncertainty in the phase of the nuclear signal after operating for a time t. Using the above relation for the signal, the variance in the phase Θ is given by

$$E(\Theta^2) = \frac{T_1 t^2}{\gamma^2 H^2 T_2^6}\left(\frac{P_N}{BP_s}\right) + \left(\frac{T_1}{T_2}\right)^{1/2} \frac{1}{\gamma H T_2}\left(\frac{P_N}{BP_s}\right) + \frac{1}{T_2}\left(\frac{P_N}{BP_s}\right) \qquad (6)$$

where P_N = total noise power
P_s = signal power

The signal-to-noise is the same as equation (3).

2.4. POSITION GYRO PERFORMANCE EQUATIONS

A complete analysis of the pulsed position gyro is given in section 6 of this report. The Arma nuclear gyro uses nuclei which have been aligned by a magnetic field to establish a position reference in space. Pulsed magnetic fields are applied, the polarized nuclei allowed to remain in a field-free environment for a period of time and then the orientation is detected.

The signal-to-noise ratio for this system is derived in a later section, however in order to simplify the calculations we have introduced two approximate relations:

$$(1) \qquad Q = 0.037 \left(\frac{W}{2\pi}\right)^{1/2} V_c^{1/3},$$

which is from Bloembergen, Purcell and Pound[4], and (2)

$$(2) \qquad L = 4\pi A^2 P^2 / V_c 1$$

which is from Abragam (Ref. 5, p. 71). With these substitutions the signal-to-noise ratio for the pulsed position gyro becomes

$$S/N = \frac{0.03 (\gamma H_s)^{7/4} \gamma (V_c)^{2/3} H_p \mu h N e^{-t/T_1} \times 10^{-8}}{k\pi^{3/4} T_b \sqrt{kT\Delta\nu}} \quad (7)$$

where
- H_s = sensing field
- H_p = magnetizing field
- V_c = volume of sample
- b = noise figure
- t = signal drift interval
- $\Delta\nu$ = bandwidth

It will be shown that the drift rate due to magnetization noise in the material is given by

$$D_p (M) = \frac{1}{t\sqrt{n}} \frac{8\pi kT}{V_c^2 T_2 h \nu H_p \eta} \left(\frac{ttc}{3N}\right)^{1/2} \quad (8)$$

where
- n = number of drift periods within the observation time
- η = enhancement factor
- t_c = critical averaging time
- t = signal drift interval

2.5. RESULTS

The signal-to-noise ratio and drift rate obtained for the various solids using the above equations is presented in section 4 of this report.

3. REVIEW OF LITERATURE

It was seen early in our program that a complete review of all literature pertaining to the nuclear magnetic resonance of solids would be necessary. The magnitudes of the various resonance properties of solids had to be known in order to perform any analytical or experimental work. Since the theory of n m r in solids is not advanced far enough for any of these properties to be calculated, they had to be obtained from actual measurements, either our own or from published results.

The properties in which we are primarily interested are the following: spin-lattice (T_1) and spin-spin relaxation times (T_2), gyromagnetic ratio, and the magnetic moment. These numerical values are necessary to determine gyro performance using the equations of section 2 of this report.

Consequently the scientific literature, both classified and unclassified, was carefully reviewed and a bibliography compiled of work performed in nuclear magnetic resonance with solids. The result of this work is listed in Appendix A. The bibliography covers the period of 1959 to the present with selected earlier references included.

3.1. THE CHOICE OF SOLIDS FOR PERFORMANCE EVALUATION

From our compilation we selected all solids which had published values for the specific properties of interest. Table I is a list of these materials showing the spin value, T_1 and T_2, gyromagnetic ratio, magnetic moment, nuclear concentration, ambient temperature and the magnitude of possible enhancement.

It should be noted that all relaxation times (T_1 and T_2) shown in Table I were determined by measurement at the given temperature T. The materials cover a wide range in relaxation time and temperature. T_2 varies from 1 microsec to 0.4 sec, T_1 varies from 0.008 sec to 18 hours and the temperature varies from 2.5° K to 750° K. The materials themselves cover a wide range of various solids, such as alkali metals, plastics, semiconductors and protons absorbed onto metal wire. For comparison, three liquids are also included in the table.

The list may seem short compared to the total amount of n m r work performed in this field. The reason is that the spin-spin relaxation time (T_2) which is of primary importance in our application is often not reported, the published research work usually having other principal goals. Of course this is not to say that every solid with known specifications has been listed. Some may have been missed in our search. However the main point is that we have listed materials with a wide range of resonance properties which will be used to evaluate gyro performance with a wide range of conditions. Any other materials within the true solid class which may be added to the list will

probably have constants which fit into the limits already considered and thus will not alter our conclusions. For a more comprehensive discussion of the intrinsic characteristics of solids reference should be made to section 5.0.

4. ANALYSIS OF NUCLEAR GYRO PERFORMANCE

The performances of the rate gyros and the position gyro were calculated for each of the materials listed in Table I. The results are presented in tabular and graphical form. For this analysis the equations for signal-to-noise ratio and directional drift given in Section 2 were used.

4.1. PERFORMANCE OF RATE GYROS

Since the signal-to-noise ratio is the same in both the Motorola and the GPI rate gyro systems, equation (3) of Section 2 was used to calculate S/N for both systems. Drift due to instrument noise in the Motorola system was calculated from equation (2) and drift due to magnetization noise was obtained from equation (4). The drift rate in the GPI system due to instrument noise was calculated from equation (6).

The following values were used for the parameters for each material in the calculations:

V_c (volume of sample) = 1 CC
F (noise figure) = 2
B (bandwidth) = 1 cps
H (magnetic field) = 2000 gauss
$R (= \gamma^2 H_1^2 T_1 T_2)$ = 1
t (drift time) = 1 hour
$h = 6.6 \times 10^{-27}$ erg-sec
$k = 1.4 \times 10^{-16}$ erg/°K
T_c = 1 sec

The value of R chosen here results in a maximum signal sensitivity.

Table II shows the results of the calculations and figures 1 and 2 represent these results in graphical form. The signal-to-noise ratio and directional drifts are plotted as a function of the ratio T_1/T_2. This ratio T_1/T_2 is taken as the independent variable only for convenience of representing the data. S/N is the signal-to-noise ratio, $D_G(N)$ is the directional drift due to instrumentation noise in the GPI scheme, $D_M(N)$ and DM(N) are the directional drifts due to instrumentation and magnetization noise respectively, in the Motorola scheme.

The signal-to-noise ratio is the same for both rate gyro schemes but the drift is different for each scheme since the signal readout instrumentation differ. The data shows a wide variation of S/N due to the wide range of temperature and relaxation times of the materials. Signal-to-noise ratio varied from a value of 1 for Si^{29} to 10^8 for solid He^3. We note that the higher S/N ratios are obtained for T_2 and T_1 equal or approximately equal

and at low operating temperatures. Thus the very poor S/N ratio of Si^{29}, Ce^{35}, P^{31} and others are attributed to the low T_2/T_1 ratio and/or high operating temperatures. Except for solid He^3 all the solids had a S/N ratio of 10^5 or less.

Similarly the drift showed a wide variation in values, ranging from 10^{-3} deg/hr for solid He^3 to 10^9 deg/hr for Si^{29}. Figure 2 shows this data plotted as a function of T_1/T_2. It is clear that most of the solids cannot be used in a nuclear gyro. Except for solid He^3, Na^{23}, Li^7 and Li^6 all the solids had drifts of 10 deg/hr or more. The alkali metals Na^{23}, Li^7 and Li^6 had drifts due to magnetization noise between .07 deg/hr to 1 deg/hr.

The calculations involving solid He^3 are based on recent measurements published in the Physical Review of January, 1963.

4.2. PERFORMANCE OF POSITION GYRO

The signal-to-noise ratio was obtained from equation (7) of Section 2, and the drift rate from equation (8). The following values of parameters were used in the calculations:

H_p (magnetizing field)	= 1000 gauss.
H_s (sensing field)	= 100 gauss.
V_c (sample volume)	= 1 cc.
t (signal drift interval)	= 0.1 T_2
b (noise figure)	= 2

The critical averaging time t_c was taken to be $\frac{1}{W}\left(\frac{T_1}{T_2}\right)^{1/2}$,

and the bandwidth $\Delta\nu$ was $1/T_2 \cdot 1/2\pi$

The results of the computation are shown in Table 2 and Figures 3 and 4. It is seen at first that the signal-to-noise ratios in this scheme are very low compared to the rate gyros for every solid except He^3. This is due to the low sensing field and long bandwidth we are forced to use in this scheme.

Drift due to magnetization in this scheme shows a similar pattern to that observed in the rate gyro systems. See Figure 4. Except for solid He^3, the alkali metals again show the smallest drift due to magnetization noise. However, the drift due to instrumentation noise is high, varying from .03 deg/hr for He^3 to much higher values. This is duc to the low signal-to-noise ratios obtained here.

4.3. PERFORMANCE OF GYROS USING LIQUIDS

For comparison purposes the performances of the rate gyros and the position gyro were calculated for three different liquid solutions. These were liquid He^3, methane doped with BDPA (bisdiphenylene phenyl allyl), and hexane doped with BDPA. The parameter values for this computation were the same used for the solids.

The results are shown in Figures 1, 2, 3 and 4 as the points 19, 20, 21. It is clear that in every case the liquids give better performance than the solids for both the rate gyro and the position gyro. This is true whether we are operating at room temperature (as with hexane) or at cryogenic temperatures. Drifts for the liquid samples were about 0.00001 deg/hr for the rate gyros to better than 10^{-6} deg/hr for the position gyro. S/N was 10^4 or better (without enhancement) for the rate gyros and 1000 or better (without enhancement) for the position gyro. An enhancement of 100 x is expected with doped methane or hexane.

4.4. REMARKS REGARDING THE ANALYSIS

The signal-to-noise ratio and drift rate computed here represents approximately the optimum values for each solid. Since S/N and drift are functions of temperature T and T_1/T_2 and since T_2 is a function of temperature, a variation of operating temperature may not improve the performance of the gyro. It is true that increasing the magnetic field H will improve our performance; however, an increase of more than 5 times for the rate schemes would be unrealistic and this would improve the gyro by about one order of magnitude. Increasing the magnitude of the magnetic fields in the position gyro system is limited due to the rapid changes of the field that are necessary. The values of H_p and H_s assumed here are realistic and could be constructed without undue difficulty.

The best signal-to-noise ratios are obtained when T_1 and T_2 are equal or approximately equal. Very low drift rates are obtained for this same condition and also when T_2 is large, i.e. when T_2 is greater than 1 sec. These conditions are, of course, satisfied by liquids where T_1 and T_2 are equal and T_2 is 1 sec or greater (550 sec for liquid He^3). For solids, only He^3 satisfied these conditions and therefore we obtain the excellent gyro performance. The alkali metals have T_2 approximately equal to T_1, however, they depart from liquid type performance by having low spin-spin relaxation times (T_2). The other solids have an extremely low T_2 and a high T_1/T_2. For example, Si^{29}, which shows the poorest performance, has T_1/T_2 greater than 10^9 and a T_2 of 0.01 msec.

TABLE I

PROPERTIES OF MATERIALS

Material	^{o}T K	I	T_2 sec	T_1 sec	γ	N	μ	η	Reference
1 H_e^3	2.5	1/2	.4	.4	$2x10^4$	$2.2x10^{22}$	$1.6x10^{-23}$	1	Solid H_e^3 (Ref. 6)
2 N_a^{23}	300	3/2	.012	.015	$6.9x10^3$	$2.5x10^{22}$	$1.1x10^{-23}$	10	Metallic N_a [redacted]
3 L_i^7	383	3/2	.040	.065	$2.5x10^4$	$4.4x10^{22}$	$1.6x10^{-23}$	1	Metallic L_i (Ref. 7)
4 L_i^6	373	1	.4	.7	$3.9x10^3$	$5x10^{22}$	$4.1x10^{-24}$	1	Metallic L_i (Ref. 7)
5 H^1	250	1/2	.006	.010	$2.7x10^4$	$6.4x10^{20}$	$1.4x10^{-23}$	1	P_a wire adsorption (Ref. 8)
6 Al^{27}	750	5/2	.001	.0025	$6.9x10^3$	$6x10^{22}$	$1.8x10^{-23}$	1	Al foil (Ref. 9)
7 H^1	300	1/2	.007	.023	$2.7x10^4$	$6.4x10^{20}$	$1.4x10^{-23}$	1	P_a wire adsorption (Ref. 8)
8 L_i^6	300	1	.1	1.0	$3.9x10^3$	$5x10^{22}$	$4x10^{-24}$	1	Metallic L_i (Ref. 7)
9 Cl^{35}	300	3/2	$.8x10^{-3}$	.022	$2.6x10^3$	$1.2x10^{22}$	$4x10^{-24}$	1	P-dichlorobenzene (Ref. 10)
10 L_i^7	300	3/2	.005	.140	$1x10^4$	$4.4x10^{22}$	$1.6x10^{-23}$	1	Metallic L_i (Ref. 7)
11 P^{31}	300	1/2	.020	25	$1.x10^4$	$3.9x10^{22}$	$5.7x10^{-24}$	1	Ref. 11
12 Al^{27}	300	5/2	$48x10^{-6}$	.008	$6.9x10^3$	$6x10^{22}$	$1.8x10^{-23}$	1	Al foil (Ref. 9)
13 H^1	4.2	1/2	10^{-6}	1.0	$2.7x10^4$	$5x10^{22}$	$1.4x10^{-23}$	50	Polystyrene with DPPH (Ref. 12)
14 F^{19}	77	1/2	$8x10^{-6}$	2.0	$2.5x10^4$	$2x10^{22}$	$1.3x10^{-23}$	1	Polytetrafluorethylene (Ref. 13)
15 H^1	77	1/2	$8x10^{-6}$	2.0	$2.7x10^4$	$12x10^{22}$	$1.4x10^{-23}$	23	Polyethylene (Ref. 14)
16 H^1	233	1/2	$5x10^{-6}$	30	$2.7x10^4$	$3x10^{22}$	$1.4x10^{-23}$	1	Ref. 15
17 Ga^{69}	77	3/2	$.43x10^{-3}$	20	$6.3x10^3$	$2x10^{22}$	$1.x10^{-23}$	1	Ga P (Ref. 16)

TABLE I

PROPERTIES OF MATERIALS

Material	$^{o}T_{K}$	I	T_2 sec	T_1 sec	γ	N	μ	η	Reference
18 S_i^{29}	4.2	1/2	10^{-5}	18 hrs	5.3×10^{3}	3×10^{22}	2.8×10^{-24}	1	S_i with P (Ref. 17)
19 H_e^{3}	3.0	1/2	550	550	2×10^{4}	2×10^{22}	1.1×10^{-23}		Liquid (Ref. 18)
20 H^{1}	300	1/2	1	1	2.7×10^{4}	6×10^{22}	1.4×10^{-23}	100	Hexane and BDPA (Ref. 19)
21 H^{1}	90	1/2	1	1	2.7×10^{4}	6×10^{22}	1.4×10^{-23}	100	Methane and BDPA (Ref. 19)

I = spin

γ = gyromagnetic ratio, rad/gauss

N = nuclei per cc

μ = magnetic moment, ergs/gauss

η = enhancement factor

Materials 19, 20, 21 are in liquid state.

TABLE II

RATE GYROS

SIGNAL-TO-NOISE RATIO AND DRIFT

Material		T_1/T_2	S/N	$D_G(N)$ deg/hr	$D_M(N)$ deg/hr	$D_M(M)$ deg/hr
1	H_e^3	1	5×10^7	2×10^{-6}	2×10^{-4}	$1.\times10^{-3}$
2	N_a^{23}	1.2	1×10^3	.2	29	.2
3	L_i^7	1.6	3.5×10^4	.1	26	1.3
4	L_i^6	1.7	1.5×10^2	.6	60	.07
5	H^1	1.7	3.5×10^2	.6	1700	7
6	Al^{27}	2.5	10^3	570	4×10^3	10
7	H^1	3.3	2×10^2	2×10^2	2600	13
8	L_i^6	10	10^2	1.7	340	10
9	Cl^{35}	28	10	6×10^5	2×10^5	5×10^2
10	L_i^7	28	3.5×10^3	11.4	210	4×10^4
11	P^{31}	1250	35	190	6×10^3	.1
12	Al^{27}	2000	1.6×10^2	190	10^4	2×10^3
13	H^1	10^6	2×10^4	3×10^9	4×10^3	5×10^4
14	F^{19}	2.5×10^6	2×10^4	6×10^{14}	2×10^4	2×10^6
15	H^1	2.5×10^6	1×10^5	2×10^7	210	5×10^4
16	H^1	6×10^6	10	2×10^{13}	10^6	10^8
17	G_a^{69}	5×10^7	2.5×10^3	6×10^5	4×10^3	10^5
18	S_i^{29}	7×10^9	1	6×10^{16}	2×10^8	3×10^9
19	H_e^3	1	3.5×10^6	5.7×10^{-7}	1.8×10^{-6}	4×10^{-5}
20	H^1	1	3.5×10^4	1.6×10^{-5}	10^{-2}	4×10^{-2}
21	H^1	1	2×10^5	4×10^{-6}	5×10^{-4}	10^{-5}

TABLE II

RATE GYROS

SIGNAL-TO-NOISE RATIO AND DRIFT (Continued)

$D_G(N)$ = Drift due to instrument noise in GPI system

$D_M(N)$ = Drift due to instrument noise in Motorola system

$D_M(M)$ = Drift due to Magnetization noise in Motorola system

TABLE III

POSITION GYRO

SIGNAL-TO-NOISE RATIO AND DRIFT

Material		T_1/T_2	S/N	$D_p(N)$ deg/hr	$D_p(M)$ deg/hr
1	H_e^3	1	$5x10^5$	.03	10^{-7}
2	N_a^{23}	1.2	.5	10^3	.07
3	L_i^7	1.6	2	10^4	$4x10^{-1}$
4	L_i^6	1.7	3	10^3	$5x10^{-3}$
5	H^1	1.7	.5	-	.1
6	Al^{27}	2.5	.1	-	20
7	H^1	3.3	.4	-	.5
8	L_i^6	10	.3	-	.03
9	Ce^{35}	28	0	-	19
10	L_i^7	28	.2	-	2.3
11	P^{31}	1250	2	10^4	.1
12	Al^{27}	2000	.1	-	100
13	H^1	10^6	2500	10	1
14	F^{19}	$2.5x10^6$	.2	-	210

TABLE III

POSITION GYRO

SIGNAL-TO-NOISE RATIO AND DRIFT (Continued)

Material		T_1/T_2	S/N	$D_p(N)$ deg/hr	$D_p(M)$ deg/hr
15	H^1	2.5×10^6	27	60	3
16	H^1	6×10^6	8	10^6	930
17	Ga^{69}	5×10^7	.3	-	70
18	Si^{29}	7×10^9	110	10^4	300
19	H_e^3	1	10^7	10^{-4}	5×10^{-9}
20	H^1	1	420	.1	10^{-6}
21	H^1	1	2500	.04	3×10^{-7}

$D_p(N)$ = Drift due to instrument noise in position gyro

$D_p(M)$ = Drift due to magnetization noise in position gyro.

5. DISCUSSION: APPLICABILITY OF SOLIDS TO THE NUCLEAR GYRO

Recent advances in the theory of the solid state have lead to the discovery of many useful properties and the development of such devices as transistors, and masers. In nuclear magnetic resonance of materials in the solid state many properties are very different from those of liquids or gases. In general these differences give poorer signal strengths and result in substantial deviations from the predictions of the theory of NMR as expressed in the classical equations of Bloch. Most notable are the extreme values of relaxation times, with the longitudinal time constant, T_1, very long and the transverse constant, T_2, very short, with large variations under changes in the D.C. magnetic field and the radio frequency field strength (Ref. 20).

5.1. RELAXATION TIMES OF SOLIDS

Nuclei in the solid state show very different behavior in nuclear magnetic resonance from the same nuclei in the liquid or gaseous state. Typical solids have the nuclei in fixed positions in the lattice, with movements restricted to vibrations about those positions. The result is a very weak coupling to the lattice because of the absence of collisions but a very strong coupling between the nuclei which are exposed to each other's field without break. Hence the typical solid has $T_1 >> T_2$. The very long persistance of magnetization, expressed as large T_1, looks at first sight very attractive for the nuclear gyro. But analysis of the instrumentation errors show that a large $\frac{T_2}{T_1}$ is needed to enable readout of the gyro signal over the noise of both the instrumentation and the nuclear magnetic backgrounds. In some cases a large T_2 is important as well. These properties are given to liquids by the Brownian movements with collisions occurring at intervals short compared to the Larmor period.

The theory of this relaxation process was worked out by Bloembergen, Purcell & Pound (Ref. 4), who were able to experimentally demonstrate its validity for many materials. Their work shows that these properties are fundamental to materials. The most interesting result is the predicted equality of T_1 and T_2 for low viscosity liquids, where the values of $\frac{1}{T_1}$ and $\frac{1}{T_2}$ are proportional to $\frac{n}{T}$, where n is viscosity and T the absolute temperature. For $\frac{n}{T}$ above a critical value, T_1 increases with increasing $\frac{n}{T}$, while T_2 continues to decrease. It is shown that the curves for T_1 and T_2 diverge at about the value of T_c, the correlation time for collision equal to the Larmor period. Solids and viscous liquids fall in the region where T_c

[redacted]

$>> \frac{1}{W}$ Larmor and can be expected to have $T_1 >> T_2$, according to the accepted theory.

The diffusible solids, N_a, etc., do not fall in the above pattern since diffusion was not considered in the theory of B P P. It is considered by H C Torrey (Ref. 21). But these materials are all only semi-solid, being very soft in the diffusible temperature range. Beyond this range they behave much like true solids both physically and in N. M. R., and the diffusible working range of temperatures is limited. Of these materials only H_e^3 has workable time constants at the temperatures of superconductivity.

5.2. GOAL PERFORMANCE VS. SOLIDS

The task of getting useful gyro performance in a nuclear magnetic resonance gyro is not easy, and may on practical grounds be too demanding of precision beyond the present state of electronic art. This demand for precision is a result of the fact that normal resonant frequencies are the order of 10^3 to 10^6 cycles as against a goal performance of 10^{-9} cycles. Since the best frequency references are barely approaching a part in 10^{12}, and some allowance is needed for instrumentation efficiency, even the advanced state of "atomic clocks" must be bettered.

The results of our analyses show at once that solids as a class fall far short of the goal performance, especially if typical solids are used. There is however, a class of materials which is usually considered solids that shows much better performance prospects. These are the elements Sodium, Lithium 6 and Lithium 7, Phosphorus (white) and Helium 3. In N M R these materials have many of the characteristics of liquids rather than solids. This peculiarity is explained by the rapid self diffusion of the nuclei in the material for a considerable range of temperatures below the melting point (Ref. 22). But in no case is there any improvement in expected performance because of the solid state. There are liquids which promise better performance in each instance. In the case of H_e^3 where the solid theoretically approaches the stated goal, an order of magnitude improvement is offered by the liquid. To solidify H_e^3 requires pressures in the range of 15 to 100 bars needing a special compression cylinder of the Bridgeman type. This added complexity reduces the possible gyro performance.

As shown in the preceding section of this report the predicted limits of accuracy have revealed no solid state materials except H_e^3 which can give drift rates much less than one degree per hour, and this includes the other diffusible solids. Typical solids fall in the range of 10 to 10^8 degrees per hour. In the case of He^3, the performance is limited by the magnetic noise, and enhancement could give a considerable improvement. However, except for optical pumping in gas at 1 mm. pressure, no success with enhancement has been reported, although considerable effort has been expended in trying

the standard techniques (Ref. 23). Note that because of its unfavorable T_1/T_2 ratio and very short T_2, Si^{29} is the poorest performer of the entire list, although it was suggested at first because of its very long T_1. Even the large enhancement possible will leave it among the poor performers.

He^3 in liquid form shows substantially better performance possibilities than the solid. Since a special high pressure container is needed to solidify the He^3 (Ref. 6) this would be a complication which produces a loss in performance. Protons in liquid hexane at 300° K or methane at 90° K show performance at goal levels (using enhancement techniques) all better than any solid now known, except He^3.

5.3. ENHANCEMENT POSSIBILITIES FOR INCREASED ACCURACY

5.3.1. Microwave Pumping in Solids

Enhancement is a very effective way of increasing the gyro accuracy capabilities. In fact it gives improvement in all the predicted performance factors proportional to the enhancement ratio. In microwave pumping this gain is theoretically limited only by the ratio of gyromagnetic ratios of electrons to the nuclei, and this number ranges from 600 to 6000. But achieved values fall far short of these large numbers. In our estimates on the list of materials only experimentally achieved factors are used, and these run from 10 to 100. But pumping cost is considerably complex, since we must pump at microwave frequencies. We note that conventional equipment for solid state enhancement requires tons of equipment. Optical pumping can be much simpler. A detailed discussion by Prof. Jeffries of dynamic nuclear polarization by microwave pumping in solids is presented in Appendix B.

Gaseous systems have been successfully pumped by optical methods. Hg vapor results are well known (Ref. 24) and recently He^3 at 1 mm. pressure showed very large polarization by simple pumping from a special lamp, as reported by Shearer, Colgrave & Walters (Ref. 25). Since the density at this pressure is about 10^{-6} that of the liquid, signal intensity comparable to liquid at Ho of 1000 gauss is obtained, but satisfactory signals can be observed at very low Ho values, giving lower observed frequency, a possible practical advantage.

This failure to get optical performance at higher concentrations is characteristic of photoluminenscence as well as this enhancement problem. Too frequent collisions result in shorter lifetimes of the energy states and conversion of the energy to other forms, which quenches luminescence and may disturb the special sequence of transitions needed for effective enhancement (Ref. 26).

5.3.2. Optical Pumping in Solids

Optical pumping might be a possible solution to the problem of adequate performance of solids. The gains made in gases look very attractive. But these gaseous systems have been made to work only at low pressure in the range of one millibar. The art of solid state masers and lasers involves pumping, often in the optical range, but this art is not applicable in its usual maser form when the goal is the pumping of unpaired electrons to produce microwave or light radiation, and such materials are paramagnetic, which seriously disturbs the nuclear processing. One must find a situation where the population in one level will build up either through selective pumping to a specific hyperfine level or a material in which the natural selection rules for spontaneous emission favor the desired population buildup, and this in a diamagnetic medium.

Added to the above conditions is the need for a suitable nuclear resonance performance. One must not increase the magnetic perturbations inside the crystal, hence one must avoid paramagnetic materials where huge fields are reported. But this is the type of material which makes the best fluorescent crystals which are used for masers and lasers and about which most information is available. There are atoms among the heavier elements, usually called transition elements, in which the inner shells of electrons are not filled. Electron transitions among these unfilled orbits give lines, both emission and absorption nearly as sharp as gas spectra. But these configurations are all paramagnetic (Ref. 27), because of the unpaired electrons. Hence in general they are not suitable for nuclear gyro use, and thus the best of the fluorescent materials are not likely candidates for use in a nuclear gyro.

An ideal material might be found as a doped crystal, with the dopants as the nuclear resonant nuclei. The matrix should be neutral magnetically. The only metallic element which satisfies these requirements is calcium. There is an isotope Ca^{39} which has a nuclear moment, but it is only 0.15% concentration and might even serve as one of the dopants. Another dopant should be found to satisfy the need for a double nuclear system (such as the GPL system), but no clues have been uncovered as to which might be suitable. It must have a gyro magnetic ratio very different from Ca^{39}, if this is used and yet show sharp enough lines to build the needed enhancement. No obvious candidate has been found. Scandium was considered as dopant because its compounds are diamagnetic but in this state it lacks the 3d electron in its only ionic state. All the well known doping materials which give line spectra rather than band spectra involve the groups of transition elements. There are 3 such groups, the iron group, from Titanium, atomic number 22 to Nickel, number 28, in which the 3d orbit is unfilled; the Yttrium, No. 39

to Rhenium No. 45, with the 4 d shell unfilled; the rare earths Cerium, 58, to Ytterbium 70, with 4 f unfilled and the actinides, Actinium, 89, to Uranium 92, with 6 d orbits unfilled.

These elements or their ions are the active elements in most fluorescent crystals, and seem to be the only ones giving line spectra. This gas-like behavior is attributed to the fact that the outer shells of valence electrons screen these inner orbits from the influence of neighboring atoms. The frequencies of these inner shells are in the visible or adjacent ultra violet regions of the spectra and so are practical to use; however, these transitions tend to be weak since they involve no change in the orbital angular momentum quantum number, ℓ , which is a forbidden transition in gasses, (Ref. 28) but only weak in solids where the degeneracy is removed by the crystal electric fields.

Another problem is the need to have a good source of light at the required frequency. In microwave pumping the oscillator can be tuned to the required frequency. But in optical pumping a natural source must be found at the needed frequency strong enough to give reasonable saturation to the desired transition. The dopant must be used at rather low concentration, or the N. M. R. line widths will be considerably broadened. Also since many fluorescent crystals lose their fluorescence at higher concentration it can be expected that high concentrations will interfere with the optical pumping, apparently by shortening the lifetime of certain energy levels. In some cases of phosphors, the optimum concentration is the order of 0.01%, with higher concentrations quenching the luminescence, especially where the iron group is used (Ref. 29). Dilution reduces the available signal strength, and so the gains of pumping must be large to overcome the dilution losses. (See Appendix C for Prof. Jeffries discussion of dilution effects.)

However, the number of possible materials is so large that the chance of exceptions to the above rules is good. A detailed study of the problems over the next few years, with the volume of new work being published might turn up a working combination for substantial optical enhancement of solid state nuclear magnetic resonance, which could make a useful nuclear gyro of some less exotic material than He^3.

6. A PULSED COIL POSITION GYRO

6.1. GENERAL

Experimental and analytical work on the behavior of nuclei subject to pulsed magnetic fields indicate that an angular readout system leading to a two degree of freedom angular position gyro can be predicated upon this behavior.

Major engineering tasks remain to be accomplished before the design can be fully defined. These arise largely from signal/noise or threshold conditions; reduction of stray external magnetic fields to an extremely low level is necessary; substantial increases in the number of active nuclei are desirable; internal noise in electronic amplifiers must be minimized. Approaches to each of these are available -- superconducting shields, use of microwave polarization techniques, amplifier band width reduction respectively. The stray field problem appears to be the most serious.

Sufficient experimental confirmation exists to allow forecasting gyro performance from the theory that has been developed. If sufficient relief from stray fields can be achieved it is predicted that doped methane at 90°K would exhibit a drift rate of less than .001 earth rate in reasonable instrumentation based on 10 second averaging.

It is the purpose of this section to describe the proposed system, present the theory of its behavior and calculations of potential performance, and to outline a program directed toward ultimate demonstration of feasibility.

6.1.1. Background

The proposed configuration appears to represent a novel concept in the instrumentation of a nuclear gyro. All previous attempts have centered on the idea of sensing directly angular rates of change, thereby leading to a pure rate gyro. The Arma nuclear gyro, however, uses the aligned nuclei of the sample to establish a position reference in space.

While investigating the Bloch instrumentation system, our attention was turned to the concept of using pulsed magnetic fields, allowing the polarized nuclei to remain in a field-free environment for a given period of time and then detecting orientation. Initial studies indicated that such a scheme might well be feasible, and subsequent experiments have tended to confirm this.

Laboratory tests have indicated that the signal output varies in a manner which may be predicted by basic theory. Tests with materials indicate that the characteristics of liquids are more suitable for this than those of solids, primarily from a superior signal strength consideration.

6.2. DESCRIPTION OF GYROSCOPE

6.2.1. Physical Description

Three coils, a material sample, and associated electronic circuitry form the heart of the system. See Figure 5. Polarization of the nuclei is accomplished by two pancake coils with a total of 800 turns which provide a field of 350 gauss when excited with a current of 30 amperes. At right angles to this is the sensing coil which consists of 40 turns wound on a 3 inch solenoid over a 12 inch length. The sensing field of 8 gauss when applied rapidly with a current of 6 amperes, is used to excite the Larmor frequency of the material sample. The sample itself is contained in a bottle 1" in diameter by 1-1/2" in length. Wound around the bottle, oriented in a direction perpendicular to both the polarizing and sensing fields, is the pick-up coil which has about 600 turns and supplies the signal output to the system.

Associated with the above coils are the required switching and amplifier circuits. Switching of the field coils is accomplished by a hybrid of solid state circuits and relays at the present time (see Figures 8, 9), although it is anticipated that all solid state switching would be used in any practical gyro. Amplifiers and filtering circuits are used to build up the output from the pickup coil and to improve the signal-to-noise ratio. Necessary to complete the gyro circuits is a phase discriminator which will sense the relative polarity of the Larmor frequency signal and hence indicate direction of rotation. See Figure 10.

A pair of large Helmholtz coils are used to cancel out the Earth's magnetic field. Due to local variations, the average residual field is of the order of 50 gammas. * A much more complete cancellation will be effected when suitable superconductive shielding is developed.

6.2.2. System Explanation

Operation of the system is accomplished by the following sequence of steps. See timing diagram, Figure 6, and vector diagrams, Figure 7.

(a) The currents to both the polarizing and sensing coils are turned on and held for a period of time somewhat greater than the relaxation time T_1. This creates magnetization vector in the material which is aligned in the direction of the polarizing field.

(b) The polarizing field is then reduced relatively slowly and the polarized nuclei swing around to line up with the direction of the sensing field.

---

* 5×10^{-4} gauss

(c) After the polarizing field has decayed completely, the sensing field is cut off very rapidly so as not to disturb the orientation of the aligned nuclei.

(d) A drift or waiting period short compared to the relaxation times T_1 and T_2 is allowed. During this period the aligned nuclei are in a nominal field-free environment and therefore serve as a space reference against any vehicle rotation. If any residual magnetic field is present, the nuclei will precess at a rate proportional to the magnitude of the field thereby causing an angular error. A very high degree of magnetic shielding is therefore required.

(e) At the end of the drift time, the sensing field is applied non-adiabatically with a rise time of the order of a few microseconds. If any vehicle rotation has occurred, an exponentially decaying Larmor free precession signal will be induced in the pickup coil. The amplitude of the signal is theoretically proportional to the sine of the angle of rotation, while the time constant of the decaying oscillation is the transverse relaxation time T_2 of the material. The Larmor frequency corresponds to the amplitude of the sensing field. At the present time the Larmor precession frequency is about 35,000 c.p.s.

(f) After the precession signal is read out to the system, the polarizing current is applied again, the magnetization vector reestablished and the above steps repeated.

All of the sequencing described above is performed automatically after the first step is initiated by a push button. In an actual system cyclic repetition would be accomplished by suitable programming. The useful output is the Larmor free precession signal appearing in the pickup coil during each cycle. This information would be fed into the vehicle navigation system and utilized according to some predetermined mathematical control function.

6.3. THEORY OF THE PULSED COIL NUCLEAR GYRO

Readout of gyro information from nuclei thru their resonance condition can be achieved thru rotational doppler or by reading an accumulated angle after some period of observation. The latter type, which we will call a position gyro readout is the type of interest to us.

In its most elementary form the position gyro is sequenced as follows:

(a) Polarization, to build a useful population of nuclei parallel (or anti-parallel) to the field.

(b) Alignment - to precisely cage the nuclei to the reference direction.

(c) Drift - to allow the nuclei to hold the direction as an inertial reference while the vehicle turns.

(d) Sensing to measure the angle accumulated during the drift, or observation period.

For efficient operation two samples will allow complete coverage of drift in two axes provided the time is divided equally between step c and steps a, b and d.

In the pulse system, there are 3 coils, mutually perpendicular. The polarizing coil A is split in two parts and set up decoupled from the sensing coil B, which is of solenoid form to give a uniform field at the sample. The coil C is wound around the sample for readout, and we will call it the pickup coil.

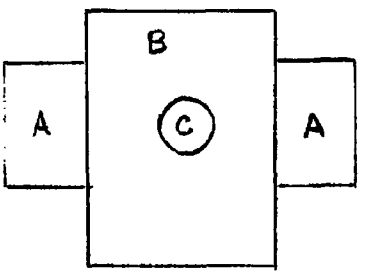

The high polarizing field needs a coil of many turns to develop fields of several hundred gauss. A pulsed RF coil colinear with the coil C will introduce RF pumping to the polarizing cycle for enhancement. During the polarizing interval the coil B is put on and left on for a few milliseconds after the polarizing current is reduced to zero. This cut off of polarizing current must be at an adiabatic rate to give a smooth approach to alignment to the sensing coil axis and not excite Larmor precession. Since the field of coil B is in the range of 10^{-20} gauss a .1 millisecond cut off rate is slow enough to satisfy the Larmor period. This swing around from coil A to coil B is not essential to the nuclear process, but solves a problem of avoiding a slow down of the cut off speed due to coupling with the large polarizing coil A, whose natural frequency is too long to allow the desired transient times.

The current in coil B is then cut off very rapidly, in one microsecond time, at least for the last part of the cut off curve. Now the nuclei find themselves aligned to the reference direction which is the axis of the sensing coil B, and exposed to a "zero" field. In the ideal case they would stay pointed in inertial space in the direction defined by the sensing coil at the instant of its cut off. Then the angle between this reference direction and the sensing coil axis would be measured.

In practice the nuclei will precess in the residual field at their Larmor rates. Since there are variations in the mean value of the local field inside the sample lattice, each nucleus will precess at its own rate determined by the sum of the residual and the local field at its position. The statistics of the local field variation are nicely shown in the NMR line shape function and more roughly in T_2. The nuclei will therefore spread out in angle as time goes on. But because the field variations are almost completely random, the large number of nuclei effectively average out the local field variations. If we run the observation time longer than T_2, the population will be reaching a condition of more or less uniform distribution over many radians, and sensitivity will be lost.

At the end of the drift period, the current in coil B is turned on, with a rise time of about 1 μ sec., to have it definitely much shorter than the Larmor precession period to make sure the start of the precession is precisely defined. Then for a time the order of T_2 one can find the initial position from the observed radiation. If we consider the X axis along the sensing coil, then rotation of the vehicle (or precession of the nuclei) around the Z or Y axis will develop an angle between the mean direction of the nuclei and the sensing axis. The precession signal will have an amplitude proportional to the sine of the accumulated angle and the phase will tell what portion of the rotation is about Z and what about Y.

To review the sequence see drawing below:

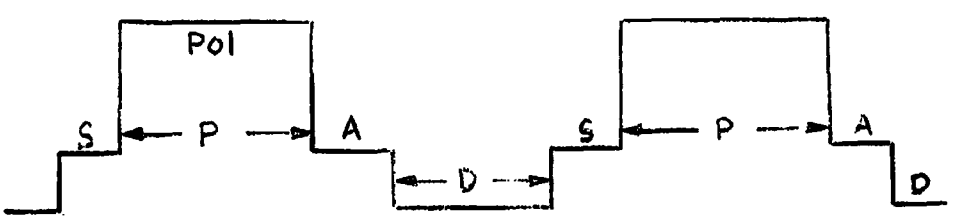

The sequence starts with the Polarizing field on interval P, then to the align (A) for a few milliseconds, then (D) for time the order of T_2 the fields are all off for 1/2 the cycle. At S the sensing field current in coil B is put on to read the output, then the cycle repeats.

The equations of motion are the Bloch equations modified to apply to the orientation system with an initial magnetization vector M_1 oriented at a small angle to the new X axis. The equations then read:

$$\frac{d\bar{M}}{dt} = \gamma \bar{M} \times \bar{H} + \hat{\imath} \frac{Mo - Mx}{T_1} - \frac{My}{T_2} \hat{y} - \frac{Mz}{T_2} k$$

$$\bar{H} = \hat{\imath} H_s$$

Further it is convenient to take $\bar{M}_1 = \hat{\imath} M_1 + \hat{\jmath} M_1 \epsilon$ allowing the drift to be a small angle ϵ around the z axis. The resulting differential equation is linear with constant coefficients.

$$\dot{M}_x = \frac{M_o - M_x}{T_1}$$

$$\dot{M}_y = \gamma M_z H_x - M_y/T_2$$

$$\dot{M}_z = \gamma M_y H_x - M_z/T_2$$

Solutions are

$$M_x = M_o - (M_o - M_1)e^{-t/T_1}$$

$$My = \epsilon M_1 e^{-t/T_2} \quad Cos \quad H_s t$$

$$M_z = \epsilon M_1 e^{-t/T_2} \quad Sin \quad H_s t$$

These equations say that the magnetization vector along the x axis shrinks from its initial value M_1 to a final value M_o exponentially with time constant T_1.

The y and z components, which couple into the pickup coil are decaying oscillations of frequency γH_s radians/second (Larmor frequency corresponding to sensing field strength). They have an exponential envelope dependent on T_2, and an amplitude $M_1 \epsilon$, proportional to the (small) drift angle ϵ and the initial magnetization. The voltage induced in the pickup coil is proportional to this amplitude.

6.3.1. Calculation of Sensitivity

This section describes our method of calculating sensitivity. The voltage induced in the pickup coil depends upon the rate of change of flux linkages with the coil, and this is calculated for a "unit angle" condition at the time the sensing coil is turned on, thus giving the "voltage/radian of drift angle during drift time" scale factor of the signal.

The noise voltage considered in this section is instrumental noise voltage arising from the coil resistance and the noise figure of the following amplifiers. Various materials and operating conditions are examined to determine the relative merits of cryogenic operating conditions in an otherwise ideal gyro.

6.3.2. Signal to Noise Ratio

The signal output of a free precession gyro sensor can be calculated in the following manner:

The magnetization is given by

$$I = 1/2 \ \mu_1 \Delta n \tag{9}$$

where μ_1 is the nuclear magnetic moment and Δ n is the excess of nuclei in state + 1/2 over those in state - 1/2.

Since at temperature equilibrium the population follows the Boltzmann distribution law,

$$\Delta n = N \ \frac{h}{KT} \tag{10}$$

where N is the total number of nuclei, h is Planck's constant, K is Boltzmann's constant, T the absolute temperature. The Larmor frequency, is given by

$$\nu = \frac{\gamma H_p}{2\pi} \tag{11}$$

where γ is the gyro-magnetic ratio and H_p is the polarizing field strength.

After the drift interval t, the population will have decreased exponentially to

$$\Delta n = \Delta n_o e^{-t/T_1} \tag{12}$$

At the time of sensing our expected population will be

$$\Delta n = N \frac{\gamma H_p h}{2\pi kT} e^{-t/T_1} \tag{13}$$

The induced flux due to the magnetization is given by $B = 3\pi I$ reduced from $4\pi I$ by the shape factor of the sample. *

The induced voltage will be

$$V = 10^{-8} F W B A p Q \tag{14}$$

where F is an efficiency factor,

$w = \gamma H_s$, the Larmor frequency in the sensing field H_s; A is the cross section area of the sample; p the number of turns on the coil and Q the gain due to tuning of the coil. The factor F makes allowance for looseness of coupling of the coil to the sample and any inefficiency in alignment or in exciting precession with the sensing field. The induced voltage is given by

$$V = \frac{3\gamma^2 H_s H_p \mu_1 h N A p Q F}{KT} e^{-t/T_1} \times 10^{-8} \tag{15}$$

Using equations (9) thru (14). This is the voltage that would be induced if the displacement angle were 90°. That is we can write

$$V = \frac{3\gamma^2 H_s H_p \mu_1 h N A p Q F}{4 KT} e^{-t/T_1} \times 10^{-8} \sin\theta \tag{16}$$

The noise voltage is given by the usual expression

$$V_{noise} = 2b \sqrt{RKT\Delta\nu} \tag{16}$$

The symbols are

R	effective resistance of coil
$\Delta\nu$	bandwidth of receiver
K	Boltzman constant
T	absolute temperature - 300°K
b	noise factor of indicating system referred to input terminals

---

* -- The number 3 is an estimate.

The calculated signal voltage for water as used without enhancement with H_p = 300 gauss and H_s = 8 gauss is 3 millivolts. We actually observe 0.25 millivolts indicating an efficiency factor of

$$F \approx 0.1$$

The noise figure of our present pickup coil and amplifier as used wide band is b = 2.4 based upon comparison of the calculated noise and observed noise. With the amplifier at 1000 cycle bandwidth this figure drops to b = 1.2. The numerical values of the constants as employed are:

μ 1 (proton)	= 1.4.4 X 10^{-23} ergs/gauss
μ 1 (sodium)	= 1.03 X 10^{-23}
h	= 6.62 x 10^{-27}
γ proton	= 2.67 X 10^{4} rads/sec
γ sodium	= 7.08 X 10^{3}
N proton	= 1.2 X 10^{24}
N sodium	= 2.3 X 10^{23}
A	= 6 cm^2
p	= 800 turns
Q	= 25
K	= 1.38 x 10^{-16} erg/°K

For a conservative estimate of the restrictions to be expected due to noise in the signal, we use the signal strengths we have observed experimentally. At the output of the preamplifier, the observed signal from protons in water, as above, was 100 millivolts peak, and the noise level of the amplifier and pickup coil was 0.97 millivolts, giving

$$\frac{S}{N} \text{ (voltage)} = 100$$

As the above was operating full bandwidth of 20,000 cycle for the amplifier and the coil at 1000 cycles width, we can reduce the noise voltage by reducing ΔV of equation (8). Because of the transient character of the output signal, we must keep enough bandwidth to avoid undue attenuation. A

figure of 8 cycles is reasonable giving an estimated reduction of the noise voltage from .97 to .035 millivolts. We expect then from protons an $\frac{S}{N}$ (voltage) = 2800.

If we can use hexane instead of water with the free radical compound 1, 3 bisdiphenylene 2-phenyl allyl (BDPA) and microwave pumping we can increase the population Δn of equation (2) by a factor of 100 as demonstrated by K. H. Hauser, Zeit fur Naturforschung, 16a, 1114, 1961. This figure can be attained with an estimated 15 watts of power at room temperatures with the doping adjusted for $T_1 = T_2 = 1$ second. We should then expect $\frac{S}{N}$ (voltage) = 280,000.

This ratio would give sensitivity adequate to detect an angular shift of 3.5×10^{-6} radian, or 0.75 seconds, since the limiting sensitivity is $\sin^{-1} \frac{N}{S}$. This sensitivity is sufficient to detect earth's rate in an observation interval of 0.05 second. Since the noise is random, a 10 second average with 0.1 second observation periods would give operation to 1/20 of earth's rate. Extension of the average to one hour gives attractive numbers, if the operating situation permits this.

Because this class of nuclear gyro is possible only with superconductive shielding, use can be made of the low temperatures for additional gains in sensitivity. With the coil at 4°K the noise as expressed in equation (16) will be reduced to 1/9 of its room temperature value.

If we assume that a parametric amplifier operating at 4°K will show a similar gain over our present preamplifier, this gain should be applicable to the entire noise term.

Doped Methane can be operated in its liquid temperature range, around 90°K and will give us an increase in useful nuclei according to equation (10) of 3X. Also it may be possible to increase the polarizing field strength but with the present uncertainty about trapped flux in the superconducting coils, we do not count on this factor. The expected cryogenic noise figure is $\frac{S}{N}$ (voltage) = 7.5×10^6.

Hence the noise in the signal will limit us to about .03 second per period, an error that is random and stationary, and will average down to the goal sensitivity in a fraction of an hour.

The use of sodium, the most suitable solid material for room temperature operation in the above calculation shows a signal strength reduction of

.01 times at constant field compared to water. This reduction is the result of the lower LARMOR frequency, of 1126 cycles per gauss instead of 4257 of protons and to the reduction of N of equation (10) to 0.19 of its value for water. The lower LARMOR frequency permits an increase in the field strengths, both H_p and H_s, of the order of 2X each, without deteriorating our non-adiabatic conditions.

This change will raise our signal voltage enough to give a predicted value of $\frac{S}{N} = 4$.

Since T_2 is only 0.01 secs and the signal will have a decay time T_2, we must keep a bandwidth of at least 30 cycles. Hence we can gain only 14X reduction in the basic noise, giving $\frac{S}{N} = 56$.

Microwave enhancement is not as effective with metals as with doped insulators because of the difficulty of achieving saturation field levels. Carver and Schlicter (Ref. 30) were able to get enhancement of 10x, with 59 watts of input power.

Assuming we can do as well, we will achieve a $\frac{S}{N} = 560$, 1/500 of the value for hexane.

The use of cryogenics with a sodium sample does not give as much help as with protons in methane, since T_2 gets very small as we lower the temperature.

Hence we must operate at 300°K for the sample, losing the temperature dependence of polarization gain.

The amplifier and coil can be operated as before however. So we can get an estimated value, $\frac{S}{N} = 5000$, for the best estimate of sodium performance. As shown in the next section this signal level will not be satisfactory for a useful gyro.

6.3.3. Required Signal to Noise Ratio

The average drift rate due to angle readout uncertainty is given by

$$\mathcal{E} = \nabla\theta / \Delta t \qquad (17)$$

where σ_θ^2 is the variance of the measured angle and Δt the time of observation or drift. Since the signal values calculated above are for the maximum which would be developed at 90° drift angle,

$$\sigma_\theta = {}^{1}/_{(S/N)} \tag{18}$$

$$\varepsilon = {}^{1}/_{(S/N)\,\Delta t} \tag{19}$$

The noise is a random quantity, hence the accumulated value of noise over k drift periods will increase by $\sqrt{k}$. But the total time will increase to k Δ t, or the signal to noise ratio for drift rate ε will be

$$\frac{S}{N} = \frac{1}{\varepsilon \Delta t \sqrt{k}} \tag{20}$$

For ε = 15°/hr., earth's rate, S/N = 1.4 X 10^4, for 10 second averaging, with 0.1 second drift intervals, suitable for proton operation with T_2 = 1 sec.

In the case of sodium, with T_2 = 0.01 secs, we must keep $\Delta t \leq 0.01$ seconds and the required S/N = 4 x 10^4 for earth's rate in a 10 second average. These numbers are summarized in Table IV.

TABLE IV

COMPARISON OF S/N FOR SODIUM AND LIQUIDS

	LIQUID (hexane)	SOLID (sodium)
INITIAL S/N RATIO		
on basis of pulsed coil instrumentation as of January 1963 prior to possible improvement	100	1.0
IMPROVEMENT		
(a) Increased field	X1	X4
(b) Bandwidth reduction in receiver	X28	X14
(c) Dynamic polarization (RF Pumping)	X100	X10

TABLE IV

COMPARISON OF S/N FOR SODIUM AND LIQUIDS (Continued)

	LIQUID (hexane)	SOLID (sodium)
IMPROVEMENT (Continued)		
(d) Cryogenic	(Methane)	
. Preamplifier and coil	X9	X9
. Polarization	X3	X1
TOTAL S/N	7×10^6	6×10^3
S/N Ratio required for earth's rate	$1.4 \times 10^{4*}$	$4. \times 10^{4**}$

6.3.4. Magnetization Noise

The previous section has indicated that the signal to noise ratio due to instrumentation admits the possibility of meeting performance goals, for example, if we use doped methane at 90°K with microwave enhancement, narrow bandwidth amplifiers and can exploit the random independent nature of the sampled noise in operating the gyro.

However, it has been pointed out that the magnetization vector and its orientation display random fluctuations due to the quantum origin of the magnetization phenomenon. Since these fluctuations constitute a background noise in which the signal is imbedded, it is conceibable that this noise source might limit performance. In this section these effects are calculated.

The effects of the basic magnetization noise (Ref. 31) have been calculated by Dodd (Ref. 2). He shows that the rate gyro is rather severly limited by these effects, which arise from the statistical fluctuations of the nuclear magnetization. Bloch indicates that the expected value of magnetic moment in zero field has a variance

$$\nabla M^2 = \mu_1^2 \, N/V^2 \qquad (21)$$

where μ is the magnetic moment of the nucleus, N the total population and V the volume of the sample. Dodd states that this value applies also to the

* -- based on 0.1 sec. sample average over 10 sec.
** -- based on 0.01 sec. sample average over 10 sec.

case when a field is present and demonstrates in the appendix of his paper that this extension is reasonable for the variance of the component in line with the magnetic field, which is the only component applicable to the rate gyro.

In the case of the pulsed coil gyro, it is the transverse component which adds to the drift rate of the gyro. But the individual nuclei are all held either parallel or anti-parallel to the field direction. Any deviation from this condition would spread the quantum energy levels, which are sharply defined. Hence in the aligned condition the transverse magnetic field has small contributions only from the permitted variations, small compared to the in-line variations. These contributions will increase as the nuclei spread out during the field free drift period, and if the period is very long compared to T_2, the nuclei will be completely dispersed in space direction giving the full predicted variance to the field component perpendicular to the original alignment direction.

Local fields (Ref. 32) are produced by the nuclear dipoles which add to the external field. These effects vary from point to point of the lattice to give the NMR line shape curves. The local field magnitudes are related to the time constant by the relation

$$\gamma \delta H = \frac{2}{\sqrt{3}} \quad \frac{1}{T_2} \tag{22}$$

where γ is the gyro magnetic ratio, δH the difference in field between the points of maximum slope for the shape curve, T_2 the spin-spin relaxation time. The averages of the local field concerned with the line narrowing are for periods comparable to $\frac{1}{W_R} = \frac{1}{\gamma \delta H}$ (Ref. 33). For a dense population of protons the local field is the order of one gauss and the critical averaging time,

$$\tau_c < \frac{1}{(W_L^2)^{1/2}}$$

The spread angle θ, will be given by

$$\theta = W_L \tau_c = \frac{2}{\sqrt{3}} \quad \frac{\tau_c}{T_2} \tag{23}$$

where now W_L is the frequency of the nuclei in the mean local field, averaged over time τ_c. Then since the spread is of the nature of a random walk, the angle θ will increase with a

factor $\sqrt{\frac{t}{\tau_c}}$ and the spread angle θ is given by

$$\theta = \frac{2\sqrt{\tau_c t}}{\sqrt{3}\ T_2} \tag{24}$$

We may refer to the ratio $\sqrt{\frac{\tau_c t}{3}}/T_2$ as the alignment factor. It represents the effort of the inertial behavior of the nuclei under classical theory. The nuclei shift from the aligned condition to the disordered field free condition only by precession in the local fields. It is assumed that the transverse noise component will grow with the spread angle. Hence an approximation for σM_{tr} the standard deviation of the transverse magnetization deviation will be

$$\sigma M_{tr} \leq 2\mu_1 \sqrt{\frac{N}{V}} \left(\sqrt{\frac{\tau_c t}{3}}\right) \frac{1}{T_2} \tag{25}$$

It is to be expected that N, the total population will be involved because the variance of the parallel nuclei adds to that of the anti-parallel nuclei, since the variance of a sum of random variables is the sum of the variances without regard to sign.

The indicated direction of the gyro differs from the true direction on account of this noise by an angle given by

$$\Delta\phi = \frac{M_{tr}}{M_z} \tag{26}$$

where M_z is the magnetization in the reference direction.

$$M_z \leq \frac{\mu_1}{2} \Delta n \tag{27}$$

where Δ n is the difference in populations of the +1/2 and -1/2 spin states. The inequalities indicated that M_z is decaying, but, in a practical time $t < T_1$, by very little.

$$\Delta\phi = \frac{4}{\Delta n\, T_2 V} \sqrt{\frac{N t\, \tau_c}{3}} \tag{28}$$

Since $$\Delta\gamma = N \frac{h\nu}{KT} E \quad (29)$$

where E is the enhancement factor. Then

$$\Delta\phi \approx \frac{4KT}{V h \nu E T_2} \sqrt{\frac{t \tau_c}{3N}} \quad (30)$$

Using the values for protons in hexane or room temperature,

ν = 1.3×10^6/sec. for 300 gauss

T = 300°K

t = 0.1 sec.

N = 1.2×10^{24}

t_c = 10^{-4} sec.

T_2 = 1 second

E = 1

h = 6.6×10^{-27} erg secs.

K = 1.38×10^{-16} erg/°

Without alignment factor,

$\Delta\phi$ = 5×10^{-6} radian, or 1 second of arc

With alignment factor

$\Delta\phi$ = 10^{-8} radian

With enhancement,

E = 100, without alignment factor

$\Delta\phi$ = 5×10^{-8} radian

With alignment

$\Delta\phi$ = 10^{-10} radian

If we employ cryogenic operation with methane and enhancement at 90°K, another factor of 3 improvement will be added due to the temperature dependence of Δ n.

With sodium, $\gamma = 6.8 \times 10^5$ for 600 gauss

$N = 2.3 \times 10^{23}$

$T_2 = .01$ second

$t = .01$ second

$T_c = 10^{-4}$ second

Without alignment factor,

$$\Delta\phi = 2 \times 10^{-5} \text{ radians}$$

With alignment factor,

$$\Delta\phi = 1.2 \times 10^{-7} \text{ radians}$$

With enhancement $E = 10$,

$\Delta\phi = 2 \times 10^{-6}$, without alignment factor,

$\Delta\phi = 1.2 \times 10^{-8}$ with alignment factor

No benefit to this term will result from cryogenics because the low temperatures reduce T_2 below useful operating ranges.

For comparison the results are as follows:

TABLE V

COMPARISON OF DRIFT DUE TO MAGNETIZATION NOISE

Material	Dodd Estimate (No Alignment Factor)	With Alignment Factor	Alignment Factor and Enhancement	Dodd Estimate with Enhancement
Hexane, 300°K	5×10^{-6} rad.	10^{-8} radians	10^{-10} rad.	5×10^{-8}
Methane, 90°K	2×10^{-6}	3.3×10^{-9}	3.3×10^{-11}	2×10^{-8}
Sodium, 300°K	2×10^{-5}	1.2×10^{-7}	1.2×10^{-8}	2×10^{-6}

The significance of these numbers is indicated in the calculations of required signal to noise ratio. Note that the merit of liquid phase relative to solid phase is clearly indicated; factors of 100:1 and 1000:1 evident for the illustrative materials.

This noise sets limits on the ultimate performance of the gyro. However, using Dodd's calculations, assuming r.f. enhancement in Hexane, we have a margin of 2000 over one earth rate when the system employs 10 second averaging. If as we have indicated, the effects of alignment are to reduce the random transverse component of magnetization, then a further reduction in threshhold by a factor of 500 is available.

Prof. Jeffries has also derived the limitations of the position gyro due to a) fluctuation in magnetization due to random relaxation, b) fluctuation in direction of the magnetization due to local fields, and c) the statistical angular spread of the magnetization due to a finite sample. This is shown in Appendix E with the conclusion that the largest effect is obtained from c), that is, the transverse component.

6.4. THE CHARACTERISTICS OF THE READOUT

We have seen that the magnitude of the output voltage is proportional to the drift angle, that is the output is an analog output.

However, all conventional gyros use an analog readout, an accuracy is not limited by this property because the system in which they are used is designed to maintain the readout as a null. The usual integrating gyro is very dependent on the excellence of maintenance of this null for its drift behavior.

In general the system requirements demand a null that is absolutely smaller as the system becomes absolutely more precise. Hence, the fractional (percent) accuracy of the readout does not need to increase as fast as system accuracy.

When the pulsed gyro is used as a null indicator in an inertial platform, the error at any time is the sum of all readouts since the reference direction was established. The summation process will average all the random type errors to a value whose deviation is given by $\sigma_\theta = \sqrt{n}\ \sigma_n$ where σ_n is the expected noise in a reading and n the number of periods summed.

The above applies to errors that are random during the mission duration. Of course, the average error is zero. Any offset errors that are steady during the mission will be compensated in the calibration procedure for the gyro system. The feedback system should hold the readout at a null by an

integrating type servo system to avoid velocity lag errors. The scaling errors in the readout are suppressed in the drift output because the null is not permitted to grow. A scaline error merely changes the servo loop again, and thus substantial scale error is tolerable.

Only the residual errors, not controllable by the above treatment, will contribute directly to the system error. An earth's rate system would need to keep a null the order of a few minutes of arc. The residual error for this system should average one second of arc, about one percent of the total null. For goal accuracy the uncompensated null should be a few seconds, with the tolerance on residual error the order of 0.01%, a difficult but not impossible task.

6.5. EXPERIMENTS CONDUCTED WITH LABORATORY MODEL PULSED COIL SYSTEM

Several experiments were conducted with various materials to verify system theory, to tune up the system and to explore relative characteristics of materials particularly as they changed from liquid to solid phase. Experiments were conducted primarily at room temperature.

6.5.1. Investigation of Null in Signal Output

A study was undertaken to investigate the null in the signal output of the Arma position gyro configuration. The pulsed coil gyro system was operating as described in section 6.2. Using protons in water or in iso-octane the system had been refined to show a signal that was about 100 times higher voltage than the basic electronic noise. Certain transients showed stronger than the noise, but were capable of further suppression with more development. But no evidence of the observability of a null suitable for a gyro readout had been collected. The next logical step was to investigate the applicability of the system by observing the null.

Methods:

1. With the Helmholz coils current set for minimum field the signal strength was observed for various values of drift time.

2. At various fixed values of drift time, the signal voltage was observed as a function of the residual magnetic field expressed as a variation in the current in the Helmholz coils.

Results:

Both tests showed a definite null in the form of a dip in output as zero drift time is approached in method (1) or as a critical value of Helmholz current was reached in method (2). The null did not go to zero in either case but this is believed the result of having control of only one compo-

nent of the residual magnetic field. In method (2), the minimum occurred at a slightly different current for each value of drift time. This shift of null position may be due to some residual of the polarizing field, which offset the alignment. The high null would be corrected when the detector is made phase sensitive. The null shift calls for a better adjustment of the decay interval for the polarizing coil. But the evidence for the useful null seems quite clear.

Conditions:

1. The polarizing coil was operated off a 50 volt supply and draws 30 amperes. It is 800 turns of wire in two square section coils, giving about 350 gauss. It is controlled by a large relay and the cut off is regulated by a shunt resistor.

2. The sensing coil is a solenoid 12" x 3" diam., of 40 turns spaced equally along the length. The current of 1.92 amps is turned on in 1 microsecond by a silicon controlled rectifier and turned off by a relay, giving about 3 gauss.

3. The sensing coil is a pie-wound 4 section coil of about 600 turns, tuned by a shunt condenser to 13 kilocycles for this test.

4. The sample, 15 cc of iso-octane, was contained in a glass tubular bottle.

5. The signal from the tuned coil was amplified by a Techtronics low noise amplifier, gain - 1000 x, bandwidth 40-40,000 cps, then filtered through a band pass filter set to pass a 500 cycle band, and the output was displayed on a Techtronics 125A oscilloscope.

   The data shown was taken with 10 seconds polarizing time to reduce variations due to the manual timing. The remainder of the cycle was electrically timed, by the sequence of relays with an electronic timer to measure out the drift interval and trigger the silicon controlled rectifier.

   It is evident from the output waveform that there is still some excitation of the pickup coil from the sensing solenoid current rise, and other later sources. These were well enough controlled for this test but need further suppression for a developed gyro system.

Data:

The data taken by method (1) is presented in Figure 11. The output reached a maximum of 4 cm deflection at 40 millisecond with the mini-

mum down to 0.9 cm at 0.5 milliseconds. This shows a rather definite null as a function of the drift time. However, this relation does not eliminate the possibility of explanation by some temporal function other than precession of the nucleii. Hence observations by method (2) were made.

Some data was taken earlier by method (2), in which a null was observed for drift times of 0.5 and 1.5 milliseconds, with observation of a definite null as a function of the residual field as controlled by the Helmholz coils. But the null vanished at higher drift times because of the poor transient conditions. These conditions were improved by readjusting the decay time constants of the polarizing and sensing coils and the null was observable up to 40 milliseconds. Figure 12(a) shows an oscilloscope trace of the output signal near its maximum value.

The maximum amplitude data are plotted in Figure 13, with Helmholz coil current as abscissa, to represent variations in the residual field. Sweeps of magnetic field were made with drift times of 0.4, 2.5, 8.0, 20 and 40 milliseconds.

It will be noted that there is still considerable output at minimum. This result is expected because the system cannot discriminate between the two degrees of freedom since it does not have its phase discriminator. Only one component of field is controlled. Also the signal polarity is lost for the same reason.

The null is shifted from the nominal zero field position which was very close to .800 amperes. This shift would correspond to an alignment offset of 1/2 radian, which would indicate some residual polarizing field at the time of sensing coil shut-off.

It is interesting that data taken at 8 millisecs was extended to .840 amp and shows a second null at .820 amp, which corresponds approximately to 180° precession from the observed null point, where another null should be expected.

It was concluded from these tests that a usable null can be developed from this position gyro configuration. The development needed includes:

1. Phase discrimination
2. Alignment precision
3. Control of output coil transient excitation

6.5.2. Experiments with Sodium, Paraffin and Polyethylene

Strong signals were observed from the prorons in water, benzene, iso-octane and even from the light oil of the sodium dispersion. But the sodium metal, which was the room temperature solid that showed the strongest signal possibility of all available solids, did not give a detectable signal. While the calculated S/N ratio for sodium is 4 (p. 31) with increased fields in the pulsed coil system, the presence of a spurious transient signal in the output coil made its observation impossible with the current state of the instrument.

This signal is shown in Figure 12(b) an oscilloscope photo, with the coil tuned to 2500 cycles. The odd shapes at the beginning of the trace is due to saturation of the pre-amplifier. The second (top) trace is of the sensing coil current. Initial amplitude is estimated at 12 millivolts, with decay time constant at 13KC of .002 second. Since the expected sodium signal is about 5×10^{-6} volts with .010 second decay constant, this signal would disappear into the background noise before the spurious signal had decayed, whereas protons in liquid give a longer lasting signal. A substantial improvement in this condition would be needed to permit finding the signal from sodium. In view of the greater difficulties of observation in solids and the poor promise of the expected results, development in this direction does not seem warranted. Signals from the sodium in the dispersion were observed on the laboratory RF NMR system.

Attention was directed to parafine and its isomer polyethylene. A report by Lowe, Bowen, and Norberg in the Physical Review (Ref. 34) indicated that T_2 for the latter material had been observed to vary from 0.1 secs in a molten sample at 392° K to 4 μ secs. in the solid at 240° K, implying a gradual change in the region near the melting point. T_1 was reported at 0.1 sec.

These materials were melted and put into the pulsed coil gyro system. In both cases, a strong signal was observed. The sample was allowed to cool gradually, and the output diminished as the material solidified. There was a lag in both samples, so that when the liquid phase was no longer visible nearly 1/2 the signal was still observed, see Figure 12 (c, d). But a few hours later, there was no detectable signal in the solid state. It was concluded from these observations that there was no intermediate value of T_2 near the melting point since there was no evidence of a shorter time constant in the oscilloscope traces.

6.6. INSTRUMENTAL PROBLEMS

The performance of the gyro has been described as a problem in signal to noise enhancement. In previous sections the noise arising from the

magnetization process, and from the elctronic instrumentation has been evaluated. Two other major areas remain for consideration. These are the elimination of stray magnetic fields which disturb the gyro during its drift period, and the technology of incorporating microwave pumping to increase the magnetization of the specimen. These latter are discussed in this section.

6.6.1. Cryogenics

6.6.1.1. Shielding

Discussions of the performance of the pulsed coil nuclear gyro have assumed that during the drift period there were no external magnetic fields acting on the nuclei. Generally speaking this will not be so. Accordingly when the sensing coil current is cut off the nuclei will go into free precession around the external residual field with a period determined by the magnitude of this field.

In order to achieve a specific level of drift rate the free precession rate must be less than the drift rate. For a drift rate of 0.001°/hour the residual magnetic field must be less than 10^{-13} gauss. To meet this requirement at the surface of the earth is a major undertaking. In a vehicle, near strong fields it will surely be more difficult. For example, in the laboratory by using Helmholtz coils we have been able to achieve a short term reduction of earth's field to about 10^{-5} gauss, and an average to about 10^{-4} gauss.

With the best high permeability shield, the multiple layer shielding, attenuation of the order of 10^4 can be achieved. It is evident that conventional techniques are not capable of giving the required degree of magnetic shielding. Superconductivity may provide the solution. A shield can 4" x 6" will show a time constant greater than 10^{14} seconds. This gives field stability for an earth's rate gyro of weeks. It can be extended to the goal performance by the help of external magnetic shielding which can limit the environmental field outside the cryogenic shield to milligauss.

A highly effective magnetic shield might be achieved by utilization of the Meissner effect in superconductors where magnetic flux is completely expelled from the interior of the superconductor. Most of the published work on the diamagnetic behavior of superconducting materials was concerned with solid samples of simple cylindrical, spherical or elipsoidal shape. Very little quantitative data was available on the diamagnetic behavior of hollow superconducting bodies such as would be required in order to create a magnetic shield for the nuclear gyro. On the qualitative side we note that it had been reported in the literature (Ref. 35) that the magnetic field inside a superconducting pure lead hollow sphere was "zero" when

measured with bismuth probes, with no comment on the probe sensitivity. The problems related to a superconducting magnetic shield include:

1. the selection and fabrication of suitable shield materials.

2. establishing methods for reducing magnetic leaks due to electrical lead connections through the magnetic shield walls.

3. Initial reduction or cancellation of stray magnetic fields prior to establishing the condition of superconductivity. This would be required in order to reduce flux trapping in the shield.

4. Measurement of extremely small magnetic fields in a liquid helium environment at approximately 4.2° K.

5. Selection of structural materials for the gyro support structure and the shield support structure. These materials must be nonmagnetic and should be capable of occasional cycling between room temperature and 4.2° K without failing catastrophically.

6. The magnetic sheld structural design should be one in which magnetic leaks due to helium gas vent ports are avoided.

Initial planning on magnetic shielding include a study of thin films deposited in high vacuum. Study of the literature revealed that the thin films have a much higher critical field, H_c, for quenching of superconductivity (i.e. reestablishment of finite resistance in specimen) than bulk materials but the diamagnetic behavior of thin films is much worse than that of bulk material (i.e. complete flux penetration occurs at very low values of field in the thin films). Perfect diamagnetic behavior of a superconductor is evident only when the dimensions of the specimen are large in comparison with the penetration depth of the magnetic field, which is of the order of 10^{-5} cm.

Inhomogeneities in crystal structure are thought to be responsible for anomalous behavior of many superconductors through a mechanism where the surface tension is lowered and it becomes energetically favorable for the metal to divide into laminar regions which exhibit an incomplete Meissner effect.

In superconduting alloys, it has been observed that a magnetic field gradually penetrates the specimen which becomes completely normal only at very high values of field. When the field is decreased, the flux remains trapped or "locked in" even at zero field. This behavior has been observed by many experimenters in tests using alloys or inhomogeneous samples of pure metals.

The considerations given above lead us to believe that the most promising approach to a superconducting shield design will be through the use of a pure, homogeneous metal such as lead which exhibits the complete Meissner effect. The critical magnetic field for lead is rather low (approximately 550 gauss at 4.2° K) but this is not an insurmountable difficulty since the shield and gyro can be designed so that the critical field is not exceeded at the shield. Lead, in addition, can be obtained in high purity form with a high degree of homogeneity and is readily fabricated. Other common elemental superconductors such as indium, tin, tantalum, niobium, aluminum, and cadmium, have been ruled out as primary choices for a shield on the basis of some or all of the following considerations:

1. Inconveniently low critical temperature.
2. Very low critical field.
3. Lack of availability in high purity, and high homogeneity.
4. Extremely difficult to fabricate.

6.6.1.2. Rotational Induced Fields in Superconductors

In London's book on Superfluids (Ref. 36) he notes that for a rotating sphere of radius R, and angular velocity w a field interior to the sphere may be induced in accordance with the equation

$$h_z = \frac{2\,mc}{e}\,W \qquad (31)$$

where m and e are the electronic mass and charge, respectively. When W is of the order of 10^3 per sec this is a field of the order of 10^{-4} gauss.

If our superconducting shield were to rotate at earth's rate we would have $W_e \simeq 10^{-4}\ \text{sec}^{-1}$

and then

$$h_{ze} = \frac{(10^{-4})\,(10^{-4})}{10^3} \simeq 10^{-11}\ \text{gauss.}$$

the equivalent precession rate corresponding to this field is determined from the sensitivity of the nucleus in the spin sample. Using 4.3 k cps per gauss we find the equivalent precession rate to be

$$We = 4.3 \times 2\pi \times 10^{3} \times 10^{-4}$$

$$= 2.7 \times 10^{-6} \text{ rad/sec.}$$

This is about one-fortieth of earth rate. It should be noted that in the planned use of the gyros the instrument actually is fixed in inertial space so that this limitation should be eliminated. In the case where the gyro is not stabilized, the effect is small enough to be compensated.

6.6.1.3. Concerning Quantized Magnetic Flux

London (Ref. 1) concluded that the magnetic flux trapped in a twofold-connected superconducting body (ring or tube) should not have any arbitrary value but should be quantized. Since this several papers have been published (Refs. 37, 38) either confirming or differing with the concept. The papers which present experimental evidence in favor of the London concept disagree with London's value of the quantized unit by a factor of one-half. London proposed a value of 4.12×10^{-7} gauss cm^2 for the unit.

If this concept of quantized magnetic flux is true and applies to a hollow sphere (with a hole in it), then our problem of proper shielding is somewhat simplified. A high order of shielding will still be necessary, however, in this section we would have to shield down to about 10^{-7} gauss instead of 10^{-13} gauss. The possibility of obtaining the very low field necessary for gyro operation thus exists.

Of course the problem of how to measure these low fields still remain. It may be necessary to employ the nuclear gyroscope itself to determine the magnitude of stray or trapped magnetic fields.

6.6.1.4. Experimental Investigations on Magnetic Shields.

D.C. Measurements

Preliminary studies on instrumentation which could be used to measure the magnitudes of extremely small magnetic fields showed that state of the art instruments available could be broadly classified according to the following types:

1. Search coils which can measure rapid fluctuations down to approximately 10^{-4} gauss.

2. Flux gate instruments which measure field values in the 10^{-4} to 10^{-5} gauss region.

3. Proton precession magnetometers which measure total fields in the 10^{-4} gauss region.

4. Solid state instruments such as Hall effect probes and bismuth resistivity probes which measure fields in the 10^{-3} gauss region.

5. Optically pumped rubidium magnetometers which can measure fields in the 10-6 gauss region.

The flux gate magnetometer instrument was selected for preliminary use on the basis of small size, ease of operation, and availability.

The D.C. measurements consisted of enclosing small iron core electromagnets in lead enclosures and periodically applying pulses of D.C. current to the coils when the enclosure was made superconductive. The penetrating field was then picked up by the flux gate magnetometer probe. Field attenuations of the order of 10^3 to 10^4 to 1 were measured with lead shields. Difficulty was experienced in obtaining sufficient resolution at these low levels since the magnetometer was subject to the very noisy magnetic environment present in the working areas. Random fluctuations in the magnetic field gave rise to similar fluctuations in the magnetometer and made detection of the field penetration very difficult.

A.C. Investigations

In order to decrease the masking effect of the random magnetic field fluctuations in the D.C. technique, an experiment was devised in which a transmitter solenoid and a receiver coil would be placed in the helium cryostat. The receiver coil was enclosed in lead and immersed in helium. The transmitter would then be energized with A.C. power while the output of the receiver would be monitored. The arrangement would more closely duplicate the proposed arrangement of the nuclear sample within a shield against external magnetic disturbances and would be less subject to slow random fluctuations in the magnetic field in the laboratory. It was expected that attenuations of the order of 10^6 or 10^7 to 1 would be readily detected by this means.

In actual experiments performed thus far, attenuations of approximately 500 to 1 have been ovserved. The reason for this unexpectedly low value have not been explained yet buy may possibly still be done to magnetic pickup in the receiver coil leads or possibly may be due to electrostatic sources of noise. Observation of the pickup coil output waveform showed an extremely distorted wave shape of the proper frequency when the shield was superconducting. The helium level was allowed to drop until a small portion of the shield was above the critical temperature for lead. At this time, the wave form changed to a pure sinusoid and the magnitude increased by approximately two orders of magnitude with further increases in the magnitude as the shield became progressively normal.

6.6.1.5. Superconductive Magnet Studies

Room temperature models of the pulsed nuclear gyro require a large solenoidal coil to produce a uniform alignment field. The power requirements of such a coil preclude continuous operation on a long term basis since the coil would overheat and be destroyed.

Superconducting magnets appear to be very desirable for the nuclear gyro application because they can be small and require little power while producing large fields.

Since the magnitude of the polarizing field is of relatively low value ($\approx$ 1000 gauss), the requirement for using high field materials such as niobium-tin or niobium-zirconium can be avoided. A readily available high purity material such as niobium is felt to be adequate for the nuclear gyro application.

Operational requirements in the pulsed mode set a switching time of approximately one millisecond for the superconducting polarizing coil. This requirement together with the relatively low field value did not pose any severe problem in coil and switching circuit design. The main problem appeared to be one of protecting the superconducting coil against catastrophic damage should the coil be driven normal inadvertently. This problem could be solved quite readily with well known techniques of using parallel copper turns as a protective energy sink. A number of wire insulating techniques are satisfactory for use at cryogenic temperatures. These include silk, formvar, epoxy or teflon cladding techniques.

An unanticipated problem which was revealed during the course of the experimental program was that of remnant flux in the solenoid with zero current through the coil. No published data on this effect had been available prior to the start of the gyro program (Refs. 34, 40). Conversations with people at M.I.T. and with various workers in the field indicated that this phenomenon of remnant flux at zero field might exist in all superconductors.

The problem of remnant flux at zero field is serious in that the flux distribution after each operational pulse will probably be nonrepeatable so that compensation techniques would not be completely successful.

An experimental arrangement was devised to obtain quantitative data on the relationship between applied field and remnant field with zero current in the coil. In this setup a search coil was rotated at high speed in the solenoid gap and the output voltage of the coil observed as a function of coil current. The coil drive was supported by teflon bearings since all other bearings would tend to freeze at liquid helium temperatures. The sensitivity of the coils was 20 mv/gauss with a resolution in the indicators of two (2)

microvolts. In practice, the stray magnetic fields which can not be compensated by Helmholtz coils set a limit of resolution of approximately 40 microvolts or an equivalent noise level of the order of 2 milligauss. Initial experiments indicated that the noise level was not exceeded by the signal from the remnant flux until the applied magnetic field was approximately 600 gauss.

A possible solution for the remnant flux might include fabricating coils of an elemental material such as lead, which shows homogeneous superconductivities in its pure form. The question of the rapidity with which this could be accomplished would require further study.

Perhaps the most serious problem in this entire domain is the evaluation of small magnetic fields. As we succeed in reducing stray fields below the threshhold of laboratory equipment we will find ourselves in a region where the only means for observing stray fields is by the free precession of nuclei in the fields - that is by means of a nuclear gyro itself.

7. SUMMARY AND CONCLUSIONS

The objective of this program was to investigate the feasibility of solids as working materials in a nuclear gyroscope, and to demonstrate this feasibility if present. Analytical and experimental work was carried out. The conclusions reached were the following:

(a) The performance of three nuclear gyro systems have been compared in an analysis of material applicability. The results indicate that solids as a class show poor gyro performance, having drift rates of approximately 0.1 deg/hr or greater. On the basis of drift performance, only one solid, helium 3, maintained under suitable conditions of cryogenic temperature and high pressures, offered a possibility of meeting performance goals of 10^{-3} degrees per hour for a Solid-State nuclear gyro.

(b) On the same performance basis liquids are superior to solids. Several liquids offer the possibility of meeting the performance without employing extraordinary environmental conditions. The liquid form of helium is superior to solid helium in this respect.

(c) Certain solids stand out as a class of materials which though inferior to liquids offer performance possibilities approximating one earth rate if used in a rate gyro system. These solids, sodium, and lithium, possess nuclear characteristics at room temperatures which approximate those of liquids.

(d) The proposition has been advanced for solids that it may be possible to find a combination of nucleus and a crystalline host which can be optically pumped to increase the effective magnetization of the susceptible nuclei. This combination has not been discovered. In certain respects the criteria for this are self-contradictory which implies a search for exceptions to the expected rules. Since this is not impossible it remains a possible avenue of solution. The doped crystal combination is proposed here as an attempt to overcome some of the problems intrinsic to solids.

(e) A new readout system has been proposed and breadboards have been made to illustrate the principle. Named Pulsed Coil Nuclear Gyroscope it is contemplated that it would be used as a two axis drift sensor on a stable platform with a pair of them forming the basis for a complete stabilization system. They also appear to be compatible in principle with a new strapped down gyroscope configuration under development for ASD. Although the design concepts for the system were oriented toward solids, operated at cryogenic temperatures, analysis and experiment indicates that this system perform poorly with solids but would be acceptable with liquid samples if certain practical difficulties could be overcome. Because of its high sensitivity to stray magnetic fields, a high order of shielding is necessary.

8. RECOMMENDATIONS FOR FUTURE WORK

1. On the basis of the current state of the art it does not appear fruitful to pursue the utilization of solids in a nuclear gyro, and based upon this we cannot recommend further investigation. However, the art does change, and new and surprising information, particularly in solid state, is continually being turned up. The one line of investigation that could be recommended is the possibility that optical pumping of some suitable nucleus dispersed in a host crystal might sufficiently enhance the magnetization to overcome the signal/noise problems intrinsic in solids and the large dilution characteristic of this structure. As noted in the text, Ca^{39} is a possible nucleus for this purpose.

2. The performance potential indicated for liquids approximates the desired goal. It is recommended that future gyroscope efforts be directed toward the use of liquid helium as the best means of achieving the drift performance.

3. All of the systems studied here have operational difficulties which must be overcome, whether solid or liquid samples are used. Since the orientation of the sensitive axis or, equivalently, the free precession in the pulsed system, is determined by the combination of controlled and stray magnetic fields all of the systems are vulnerable to stray fields and a very high order of isolation is necessary. This and the availability of a suitably stable frequency reference probably set the practical limits of performance and define the major elements of cost in these systems. They appear to represent the areas of instrument development which should be emphasized at this time.

4. The difficulty involved in shielding the sample from trapped magnetic fields may be somewhat relieved if it is true that in certain cases the magnetic field is quantized in units of about 10^{-7} gauss. This latter point is not completely accepted as a fact and this is a problem which should be pursued and settled in the future. Whether the magnetic field is quantized or not, the shielding problem is still present; however, the existence of quantized units imposes less stringent requirements on the design.

REFERENCES

1. GPI Report No. A22-1 WADD-TN-60-120, Confidential Report, March, 1960.
2. Tech Report Bell Helicopter Sub Contract No. FW-2801 Motorola, Inc. Report No. RL-TR-3846-4, April, 1962.
3. Phys. Rev. 98, 1787, 1955.
4. Phys. Rev. 73, 679, 1948.
5. Abrigam, A. The Principles of Nuclear Magnetism, 1961, Oxford Univ. Press, N. Y.
6. Phys. Rev. 129, 630, 1963.
7. Phys. Rev. 98, 1074, 1955.
8. Phys. Rev. 86, 745, 1952.
9. Phys. Rev. 113, 1462, 1959.
10. J. Chem. Phys. 29, 804, 1958.
11. J. Chem. Phys. 37, 2575, 1962.
12. C. R. Acad. Sci. 248, 1803, 1959.
13. J. Chem. Phys. 27, 115, 1957.
14. Sov. Physics, Solid State 3, 2541, 1962.
15. Phys. Rev. 114, 1219, 1959.
16. J. Phys. Chem. Solids 21, 210, 1961.
17. C. R. Acad. Sci. 247, 2337, 1958.
18. Phys. Rev. 115, 1415, 1959.
19. Zeit fur Naturforschung 16a, 1114, 1961.
20. Abragam, A. Op. cit. p. 354.
21. Phys. Rev. 92, 962, 1953.

REFERENCES (Continued)

22. Abragam, A. Op. cit. p. 517, 439, 458.

23. Redfield, A. G. Private Communication

24. Rev. Mod. Phys. 25, 174, 1953.

25. Phys. Rev. Litt. 10, 108, 1963 and Jeffries, C. D. Private Communication.

26. Prigsheim, Fluorescence & Phosphorescence, Interscience Pub, 1949, 1.285.

27. Amer. Inst. Phys. HBK. Mc Graw-Hill 1957. Sec 5-236.

28. Mc Clure, Spectra of Ions in Crystals, Solid State Phys., Seitz & Turnbull eds., 9, Acad. Press, N. Y. p. 400.

29. Prigsheim, Op. cit. p. 525, 285.

30. Phys. Rev. 102, 957, 1956.

31. Phys. Rev. 70, 460, 1946.

32. Abragam, A. Op. cit. p. 97, 459.

33. Ibid, p. 425.

34. Phys. Rev. 100, 1243A, 1955.

35. Phys. Rev. 85, 104, 1952.

36. London, F. Superfluids, Vol. I (John Wiley & Sons, New York, 1950), pp. 78 - 83, 152.

37. Phys. Rev. Letters, 7, 43, 46, 50, 51, 1961.

38. Brill. Am. Phys. Soc. 6, 121, 1961.

39. Brill. Amer. Phys. Soc. 7, 408, 1962.

40. App. Phys. Letters, 1, 41, 1962.

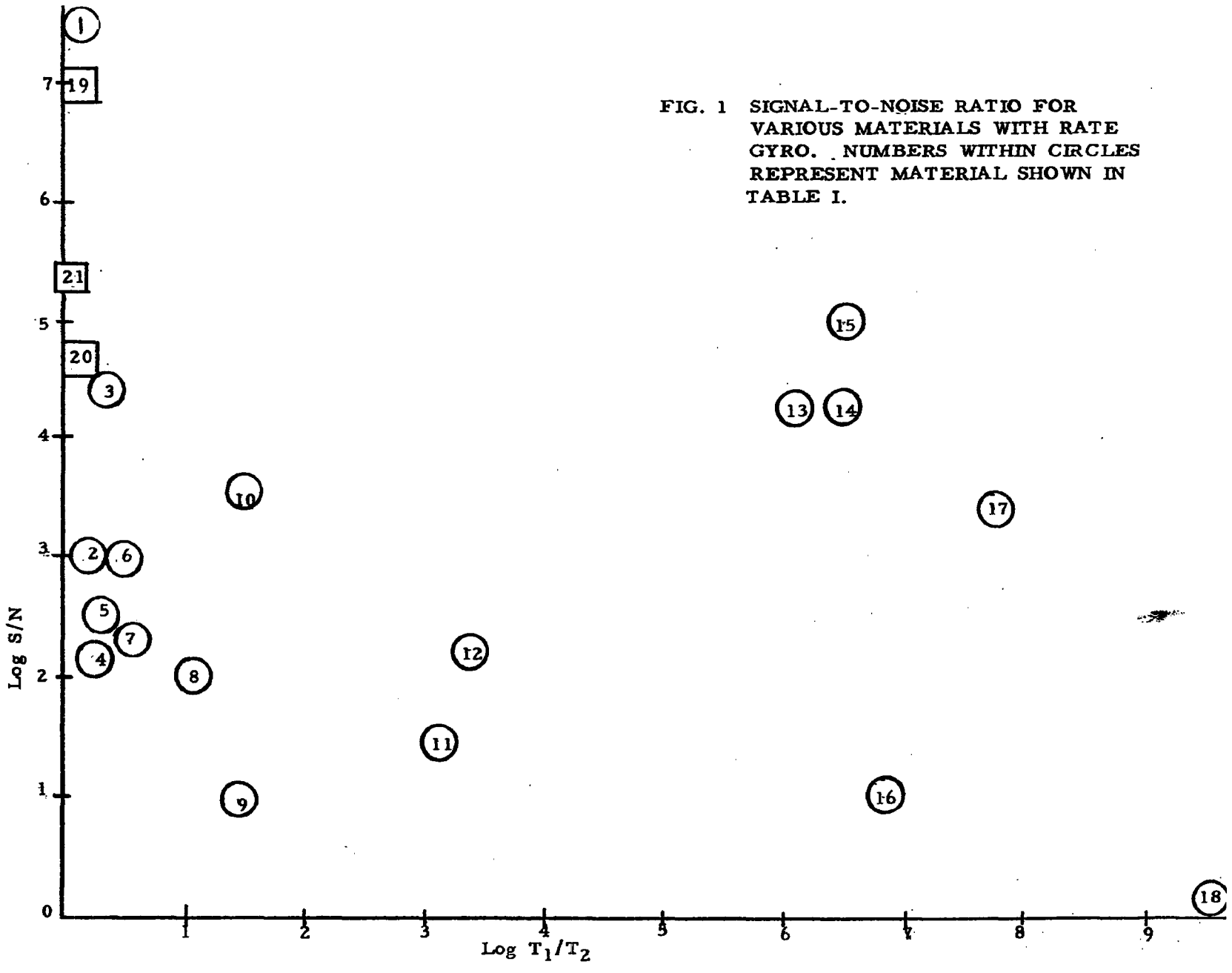

FIG. 1 SIGNAL-TO-NOISE RATIO FOR VARIOUS MATERIALS WITH RATE GYRO. NUMBERS WITHIN CIRCLES REPRESENT MATERIAL SHOWN IN TABLE I.

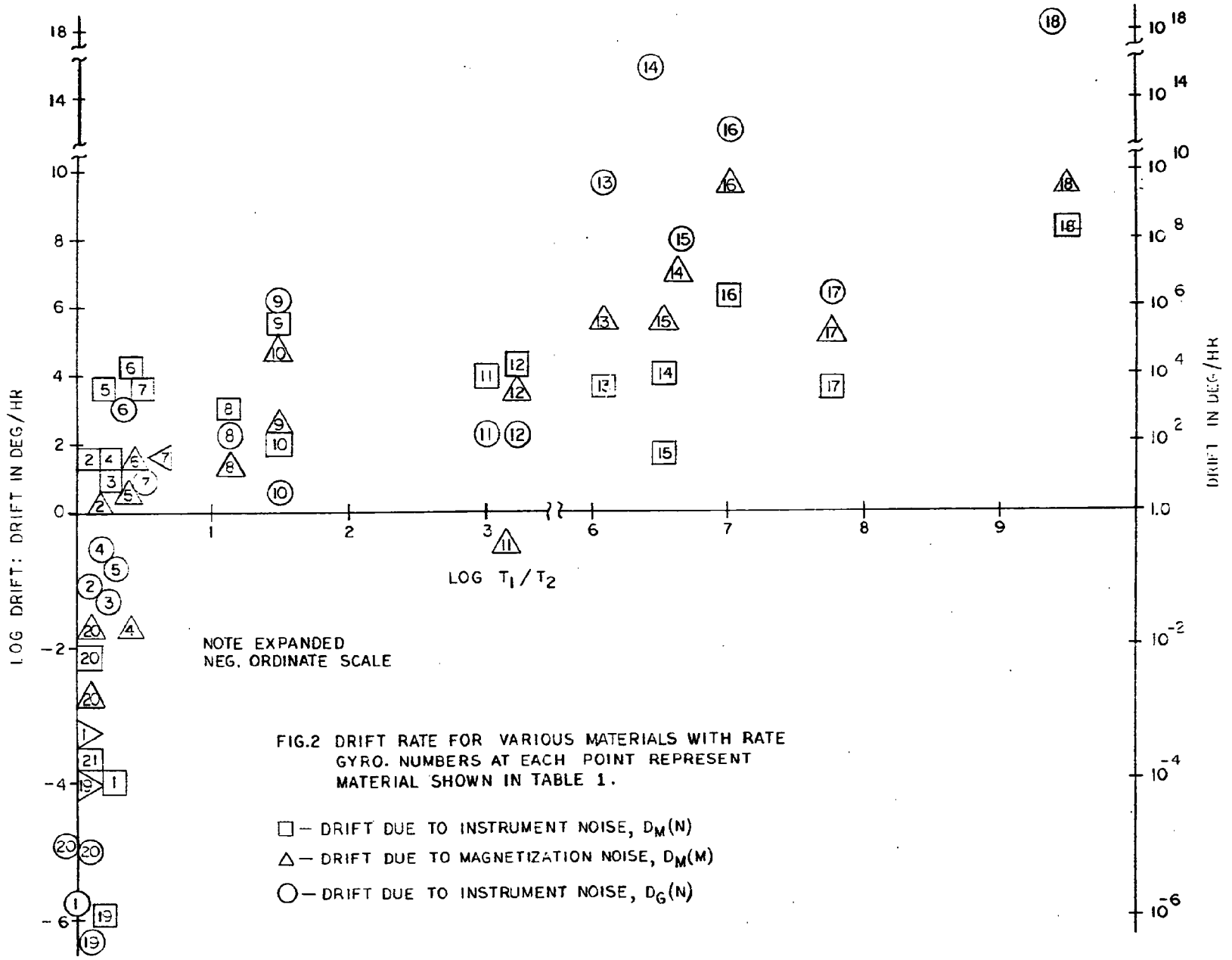

FIG.2 DRIFT RATE FOR VARIOUS MATERIALS WITH RATE GYRO. NUMBERS AT EACH POINT REPRESENT MATERIAL SHOWN IN TABLE 1.

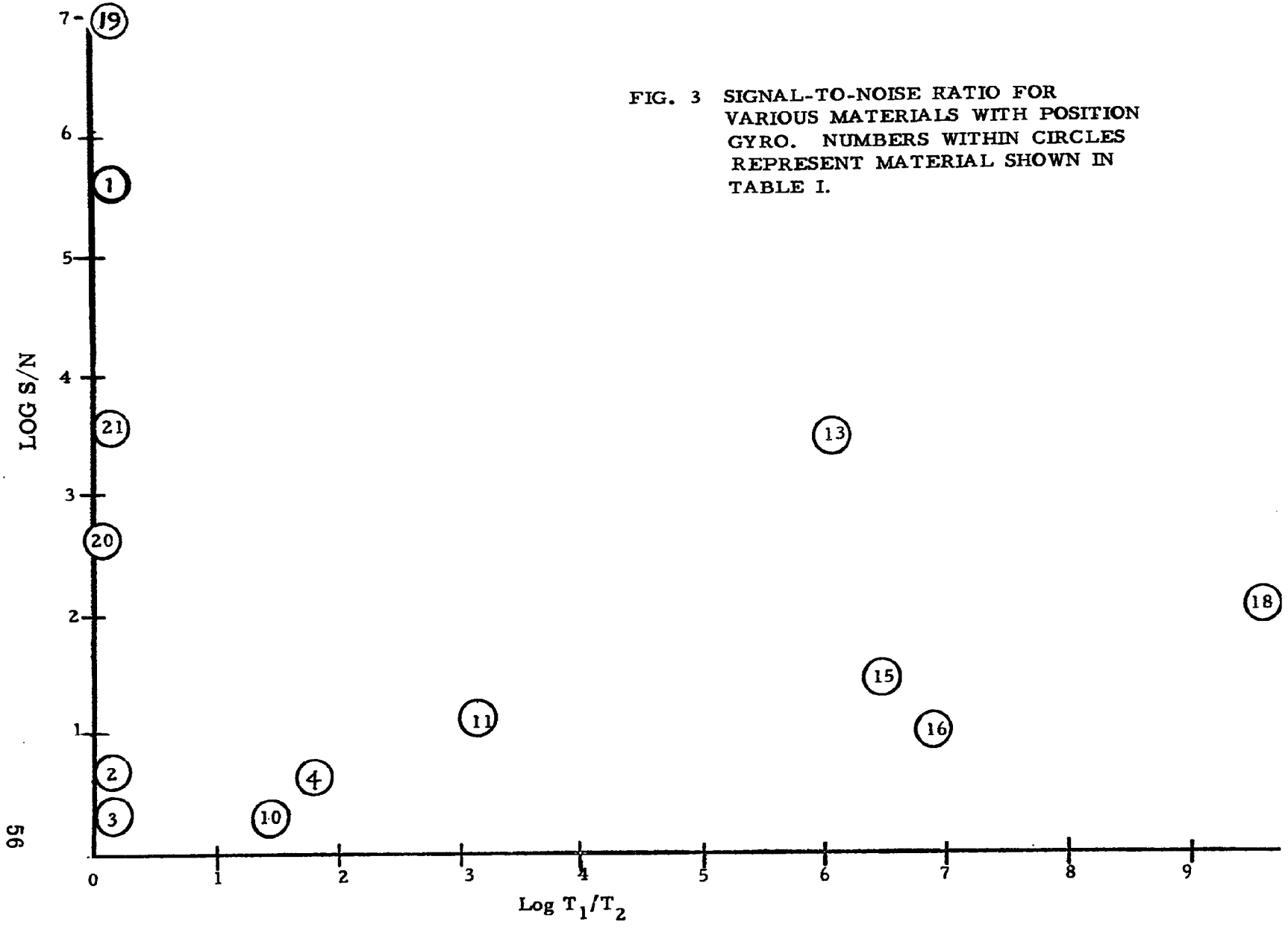

FIG. 3 SIGNAL-TO-NOISE RATIO FOR VARIOUS MATERIALS WITH POSITION GYRO. NUMBERS WITHIN CIRCLES REPRESENT MATERIAL SHOWN IN TABLE I.

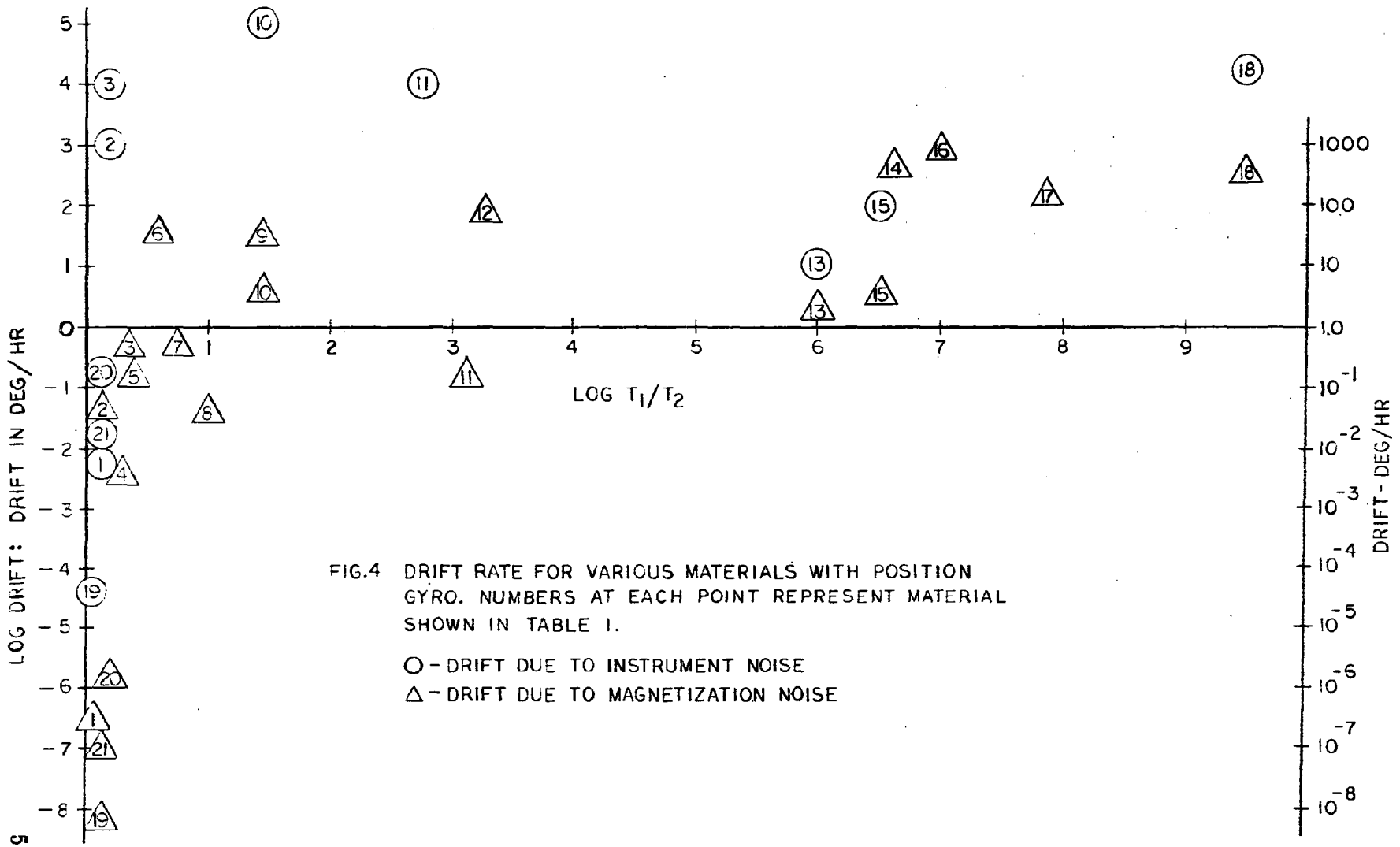

FIG.4 DRIFT RATE FOR VARIOUS MATERIALS WITH POSITION GYRO. NUMBERS AT EACH POINT REPRESENT MATERIAL SHOWN IN TABLE I.

○ - DRIFT DUE TO INSTRUMENT NOISE

△ - DRIFT DUE TO MAGNETIZATION NOISE

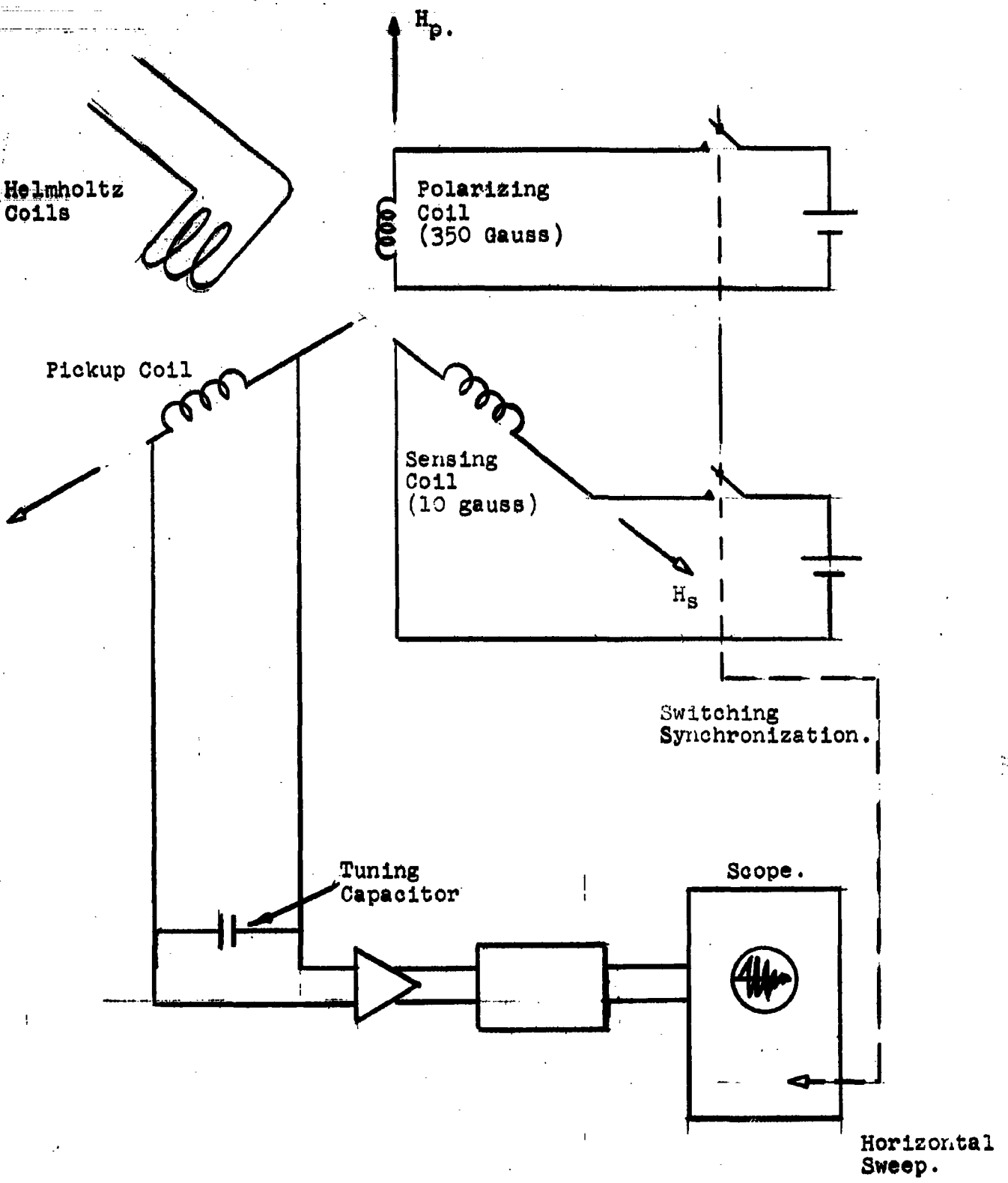

Figure 5.

Block Diagram - Pulsed Coil Nuclear Gyro.

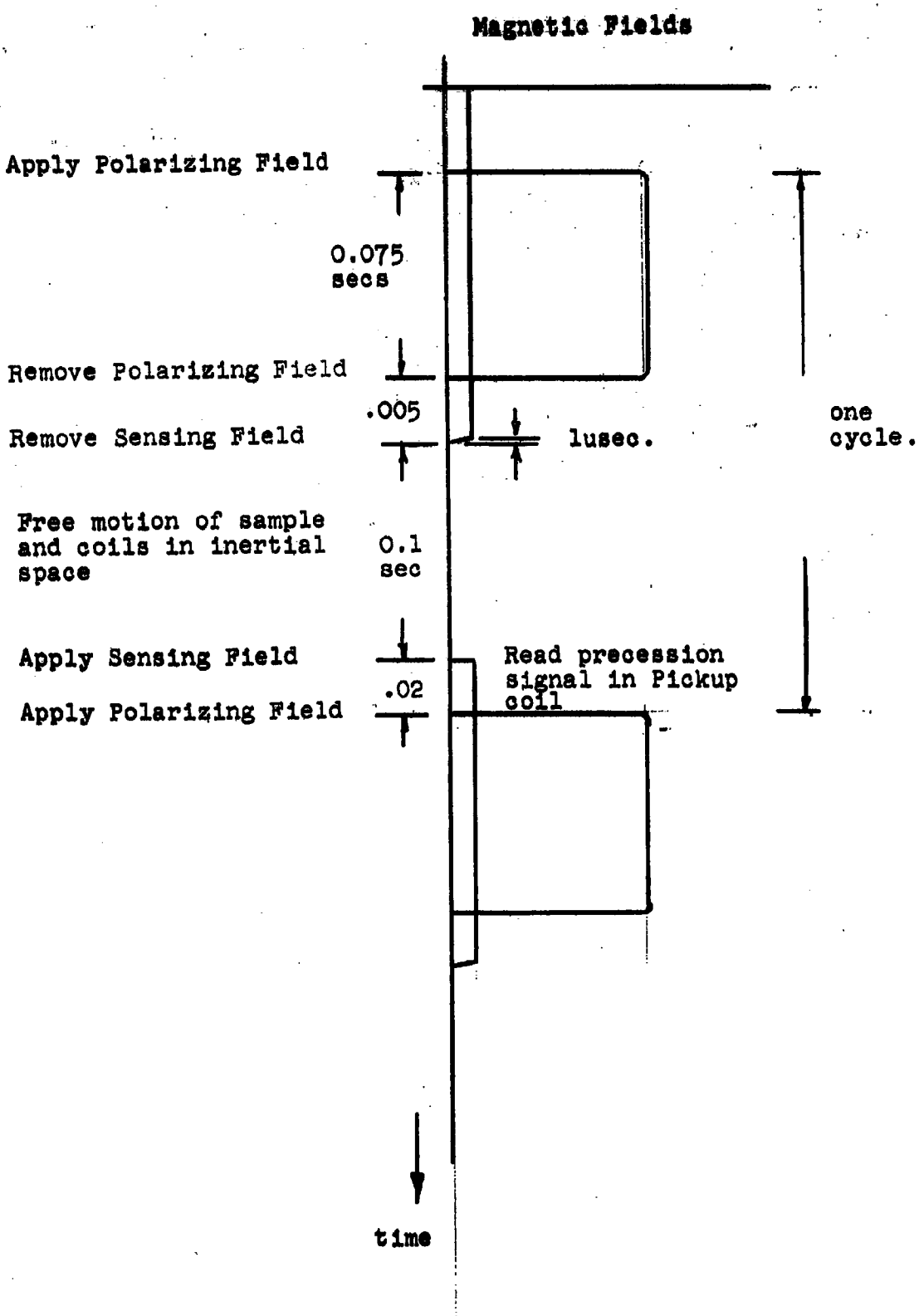

Figure 6- Timing Diagram

59

Figure 7. Operation Sequence of Applied Fields

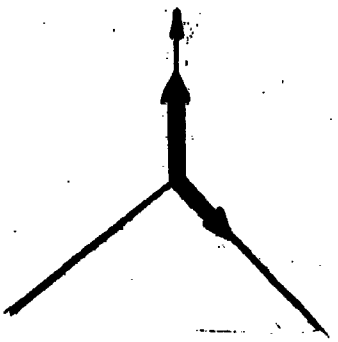

Step 1. Polarize

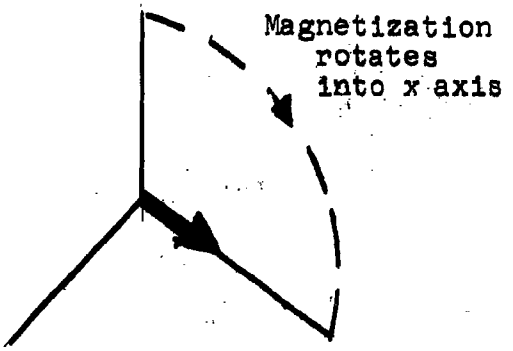

Step 2. Remove H

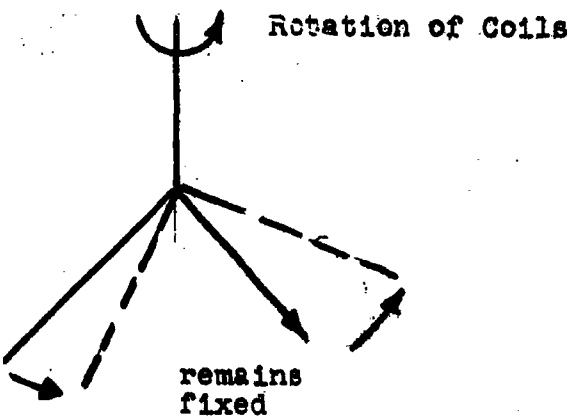

Step 3. Remove Sensing field and let nuclei drift.

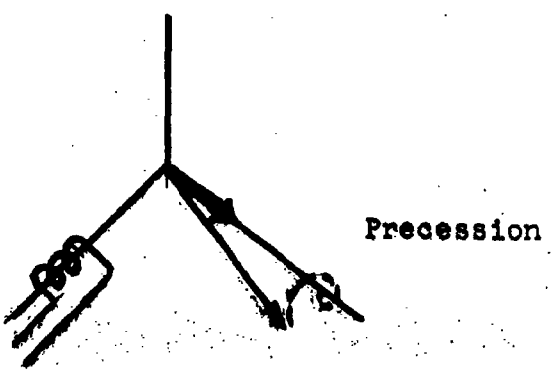

Step 4. Apply sensing field suddenly and set nuclei into free precession around x

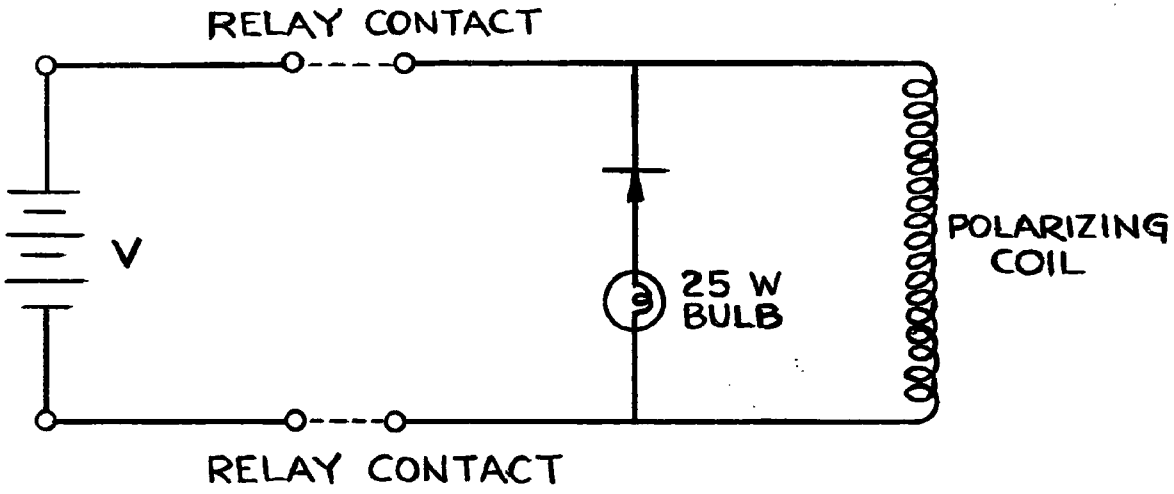

FIG. 8 POLARIZING COIL CIRCUIT

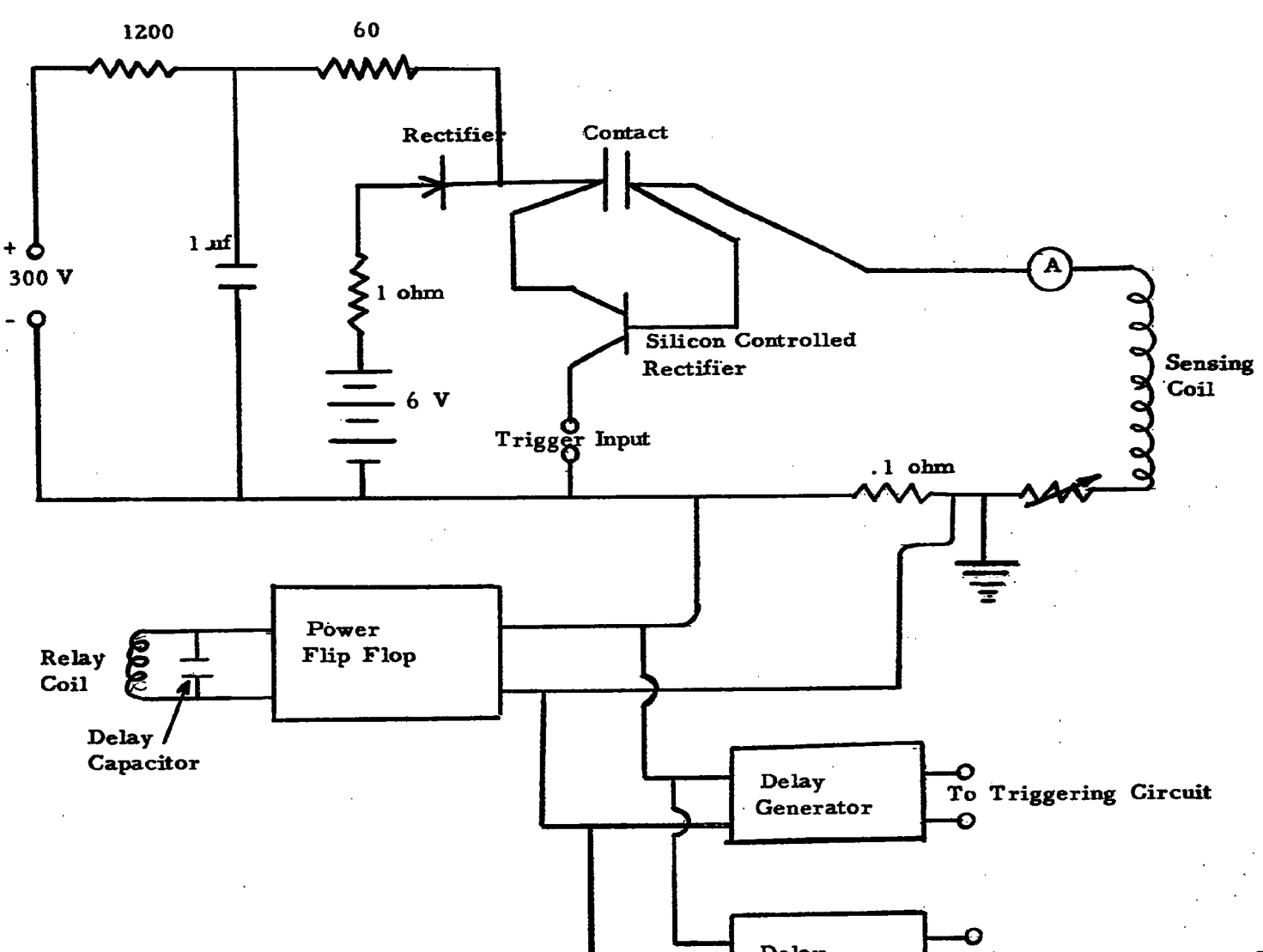

FIG. 9 SENSING COIL CIRCUIT

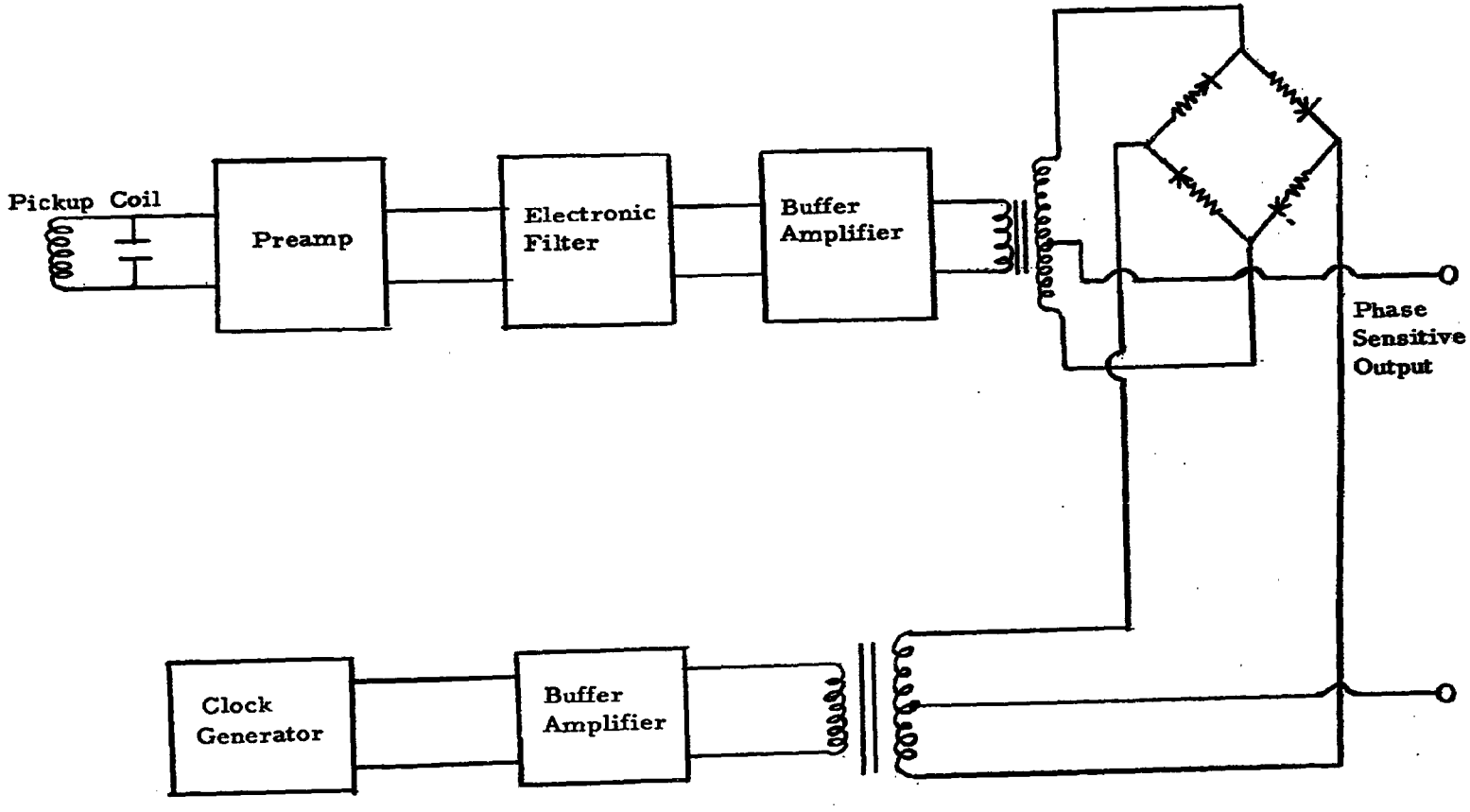

FIG. 10 PHASE DETECTION SYSTEM

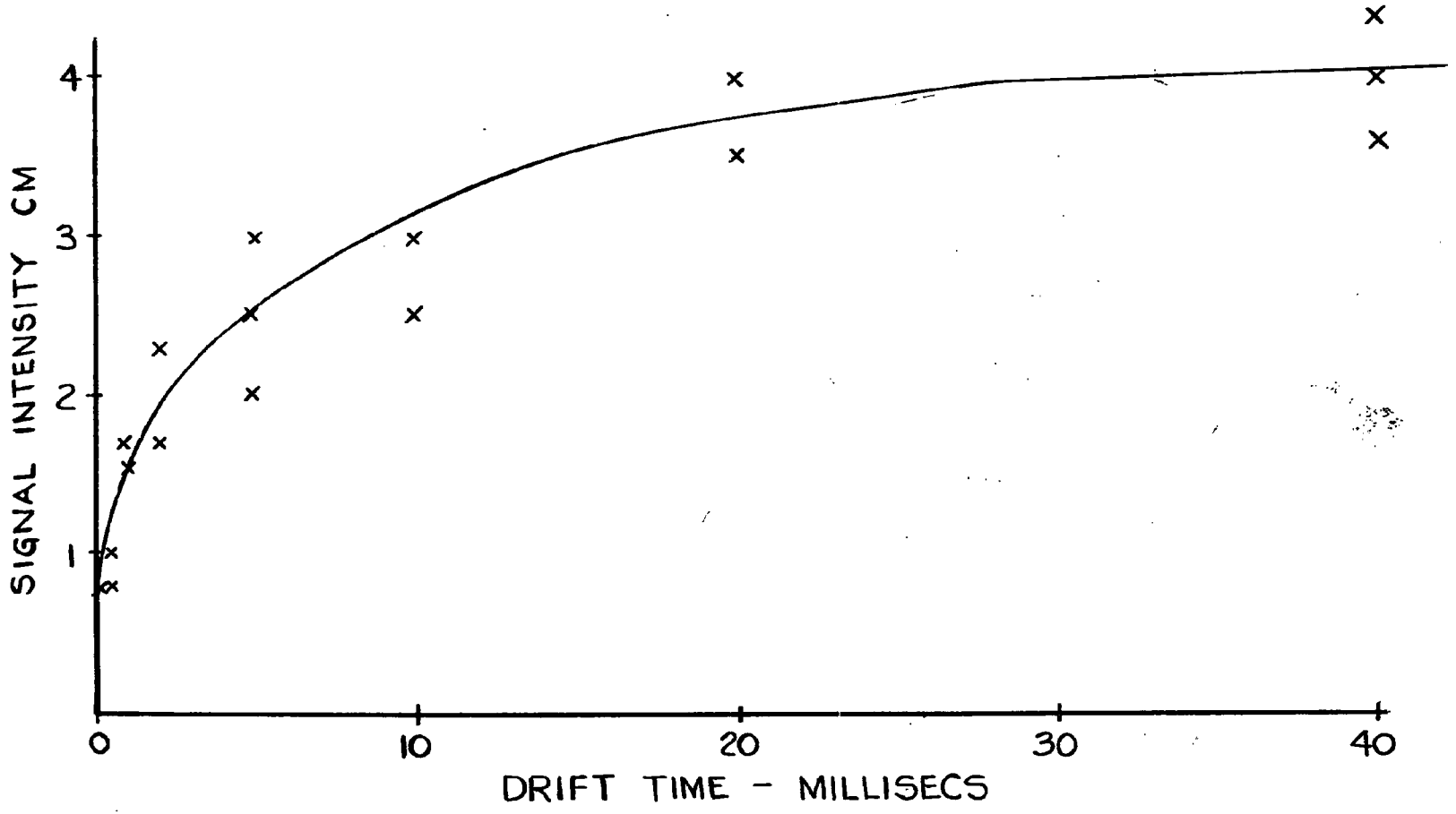

FIG. 11 SIGNAL VARIATION WITH DRIFT TIME

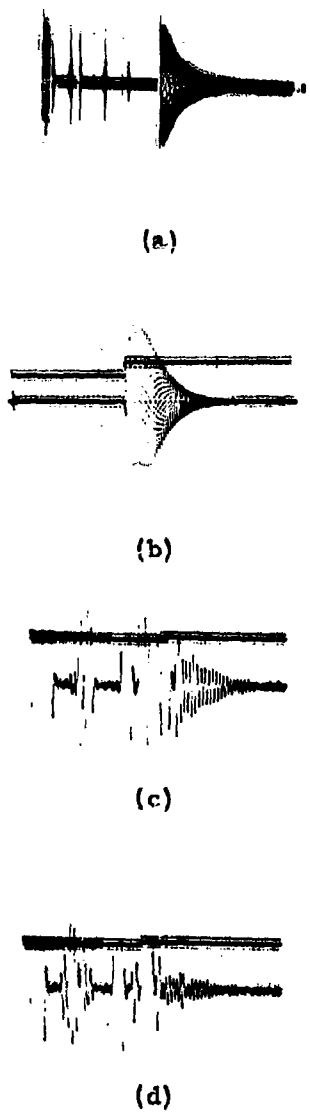

FIGURE 12 Signals obtained after sensing field H_g is applied. (a) Iso-octane sample (b) Pulse excited coil oscillation (c) Molten sample of paraffin (d) Paraffin sample which appears solid.

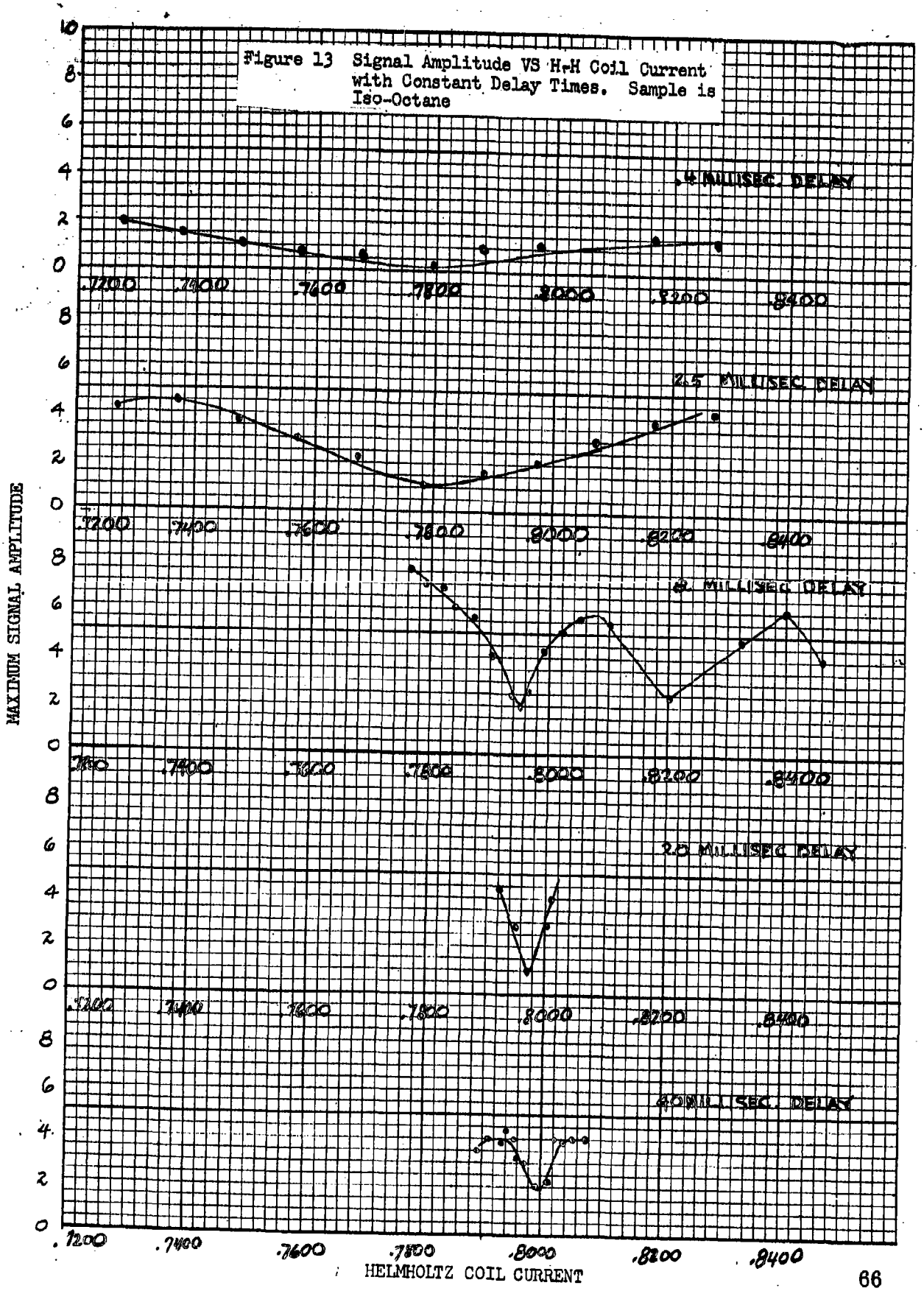
Figure 13 Signal Amplitude VS H-H Coil Current with Constant Delay Times. Sample is Iso-Octane
.4 MILLISEC. DELAY
2.5 MILLISEC. DELAY
2.0 MILLISEC DELAY
4.0 MILLISEC. DELAY
MAXIMUM SIGNAL AMPLITUDE
HELMHOLTZ COIL CURRENT
.7200
.7400
.7600
.7800
.8000
.8200
.8400

APPENDIX I

Bibliography - Nuclear Magnetic Resonance in Solids

(Period covered from 1959 to the Present plus selected earlier references)

Books

Abragam, A.
The principles of nuclear magnetism, 1961. 613 pp. Oxford University Press, N. Y.
Reviews in detail principles and presents experimental evidence of nuclear magnetic resonance.

Andrew, E. R.
Nuclear magnetic resonance. 1955. 265 pp. Cambridge University Press, London, England.

Bair, E. J.
Introduction to chemical instrumentation. 1962. 349 pp. McGraw-Hill Book Co., N. Y.
Sub-Chapter: "Nuclear magnetic resonance", p. 68-75, reviews briefly principles and apparatus.

Brand, J. C. D. and Speakman, J. C.
Molecular structure. The physical approach. 1960. 300 pp. Edward Arnold (Publishers) Ltd., London, England.
Chapter: "Nuclear resonance spectra", p. 99-125, reviews principles of nuclear magnetic resonance.

Brooks, H., Editor
Advances in semi-conductor science. The proceedings of the Third International Conference on Semi-Conductors, held at the University of Rochester, U. S. A., August 18-22, 1958. 1959. 553 pp. Pergamon Press, Ltd., London.

The following papers discuss nuclear magnetic resonance:

E. H. Rhoderick: "Nuclear magnetic resonance studies of doped III-V compounds, p. 498-504.
O. Kraus: "Nuclear magnetic resonance in semi-conductors", p. 504-506.

Clark, G. L.; Editor
Encyclopedia of spectroscopy. 1960. 787 pp. Reinhold Publishing Corp., New York.
Section: "Nuclear magnetic resonance spectra", p. 664-674 is divided into two sub-sections: "Analytical applications", by N. F. Chamberlain, p. 664-670, and "Instruments and theory", by G. L. Clark.

Clark, W. G.
Pulsed nuclear magnetic resonance in alkali halides. June 1961. 134 pp. May be obtained from the U. S. Department of Commerce, Office of Technical Services, Washington, 25, D. C. as Report No. AD-267593. Price: $4. 60

Dekker, A. J.
Solid state physics. 1957. 540 pp. Prentice-Hall, Inc., Englewood Cliffs, N. J.
Sub-section: "Nuclear magnetic resonance", p. 505-514, reviews briefly the theory.

Dodd, E. E.
Nuclear magnetic resonance rate gyro performance. April 1962. 83 pp. May be obtained from the U. S. Department of Commerce, Office of Technical Services, Washington 25, D. C. as Report No. AD-257819. Price: $8. 10

Emeleus H. J. and Sharpe, A. G., Editors
Advances in inorganic chemistry. vol. 4. 1962. 344 pp. Academic Press Inc., N. Y.
Chapter: "The use of nuclear magnetic resonance in inorganic chemistry", by L. L. Muetterties and W. D. Phillips, p. 230-292.

Englert, G. and Volpicelli, R.
Improvement of a broad-line nuclear magnetic resonance spectrometer. Feb. 1962. 25 pp. May be obtained from the U. S. Department of Commerce, Office of Technical Services, Washington 25, D. C. as Report No. AD-274519. Price: $4. 60

Frechette, V. D., Editor
Non-crystalline solids. 1960. 536 pp. John Wiley & Sons, Inc., N. Y.
Chapter: "Magnetic resonance studies of glass", by C. P. Slichter, p. 199-228; discussion, p. 228-231, discusses use of nuclear magnetic resonance for the study of local fields in the sample, with the special aim of studying structure and chemical bonding.

Gibson, A. F., Editor
Progress in semi-conductors. vol. 6. 1962 322pp. John Wiley & Sons, Inc., N. Y.
Chapter: "Magnetic resonance in semi-conductors", by J. S. Van Wieringen, p. 199-231, includes reviews of nuclear magnetic resonance effects.

Gutovsky, H. S. and Nachod, F. C.
Nuclear magnetic resonance. (New York Academy of Sciences. Annals, v. 70, Art. 4, 1960, 164pp.)

Jackman, L. M.
Applications of nuclear magnetic resonance spectroscopy in organic chemistry. (International Series of Monographs on Organic Chemistry, Vol. 5.) 1959. 144pp. Pergamon Press, N. Y.

Kopfermann, H.
Nuclear Moments, Academic Press, N. Y., 1960

Lark-Horovitz, K. and Johnson, V. A.
Solid state physics. Part B: Electrical, magnetic and optical properties. (Methods of Experimental Physics, vol. 6) 1959. 416pp. Academic Press Inc., N. Y.
Sub-section: "Resonance phenomena", by A. F. Kip, p. 227-243, reviews principles and techniques.

Meiboom, S. and others
Research in the general field of exchange kinetics: investigation of fast protolysis reactions by nuclear magnetic resonance technique. July 1959. 35pp. May be obtained from the Library of Congress, Photoduplication Service, Publications Board Project, Washington 25, D. C. as Report No. PB 142163. Price: Microfilm-$3.00
Photoprints-$6.30

Mulay, L. N.
An improved nuclear magnetic resonance apparatus and study of sandwich compounds. May 1957. 64pp. May be obtained from the Library of Congress, Photoduplication Service, Publications Board Project, Washington 25, D. C. as Report No. PB 136419.
Cost: Microfilm - $3.90
Photoprints - $10.80

NMR and EPR spectroscopy. Papers presented at Varain's Third Annual Workshop on Nuclear Magnetic Resonance and Electron Paramagnetic Resonance, Palo Alto, California. 1960. 315pp. Pergamon Press, N. Y.

Newstein, M.
Research on nuclear magnetic resonance techniques. Final report. April 1959. 103pp. May be obtained from the Library of Congress, Photoduplication Service, Publications Board Project, Washington 25, D. C. as Report No. 140624.
Price: Microfilm - $5.70
Photoprints -$16.80

22. Pople, J. A., Schneider, W. G. and Bernstein, H. J.
High-resolution nuclear magnetic resonance. 1959. 501pp. McGraw-Hill Book Co., N. Y.
Reviews in detail developments since 1945. The book is divided into two parts: Part 1 discusses the basic principles of the subject and the nature of the apparatus used, and Part 2 surveys the applications to chemical problems.

Roberts, J. D.
An introduction to spin-spin splitting in high-resolution nuclear magnetic resonance spectra. 1961. 116pp. W. A. Benjamin Publishers, Inc., N. Y.

Rowland, T. J.
Nuclear magnetic resonance in metals. (Progress in Materials Science, v. 9., No. 1, 1961, 91pp.)
Reviews of theory and experimental results.

Rutgers State University
A study of the properties of matter by means of nuclear magnetic resonance. Jan. 26, 1960. 22pp. May be obtained from the Library of Congress, Photoduplication Service, Publications Board Project, Washington 25, D. C. as Report No. PB 164334. Price: Microfilm - $2.70
Photoprints - $4.80

Sagalyn, P.
Use of nuclear magnetic resonance for radiation effects studies. July 1958. 12pp. May be obtained from the Library of Congress, Photoduplication Service, Publications Board Project, Washington 25, D. C. as Report No. PB135102.
Price: Microfilm - $2.40
Photoprints - $3.30

Schone, H. E.
Nuclear magnetic resonance in metal single crystals. Aug. 1962, 7pp. May be obtained from the U. S. Department of Commerce, Office of Technical Services, Washington 25, D. C. as Report No. AD 285023. Price: $1.00

Seitz, F. and Turnbull, D. Editors
Solid state physics. Advances in research and applications. vol.2. 1956. 468pp. Academic Press, Inc., N. Y.
The following two chapters review theoretical developments and experimental techniques in the field of nuclear magnetic resonance:
G. E. Pake: "Nuclear magnetic resonance", p. 1-91.
W. D. Knight: "Electron paramagnetism and nuclear magnetic resonance in metals", p. 93-136.

Slichter, C. P.
Principles of magnetic resonance. 1963. 246pp. Harper & Row, N. Y.

Stanford, E. G. and Fearon, J. H., Editors
Progress in non-destructive testing. vol. 1. 1959. 267pp. The Macmillan Co., N. Y.
Paper: "Nuclear magnetic resonance and its application to the testing of materials", by L. E. Drain, p. 227-263. Reviews principles of nuclear magnetic resonance and describes a number of applications to non-destructive testing.

Webb, M. B.
Nuclear magnetic resonance study of metals and alloys. Final Report. Oct. 1960. 26pp. May be obtained from the U. S. Department of Commerce, Office of Technical Services, Washington 25, D. C. as Report No. PB 157517. Price: $2.60

Wiberg, K. B. and Nist, B. J.
The interpretation of NMR spectra. 1962. 592pp. W. A. Benjamin Publishers, Inc., N. Y.

PERIODICAL REFERENCES

1963

Blume, R. J.
Demonstration of nuclear magnetic resonance in cobalt with a "grid dip" meter. (American Journal of Physics, v. 31, Jan. 1963, p. 58-59.)

Boyd, E. L.
Temperature dependence of nuclear magnetic resonance of Fe^{57} in magnetite. (Physical Review, v. 129, March 1, 1963, p. 1961-1964.)

De Gennes, P. G. and others
Nuclear magnetic resonance modes in magnetic materials. (Physical Review, v. 129, Feb. 1, 1963, p. 1105-1115.)

Drain, L. E.
Nuclear magnetic resonance in platinum. (Journal of Physics and Chemistry of Solids, v. 24, March 1963, p. 379-382.)

Litster, J. D. and Benedek, G. B.
Observation of the Nuclear Resonance in Ferromagnetic Iron to 65000 Atmospheres, JAP Vol. 34, no. 3 (March 1963).

Pedersen, B. and Holcomb, D. F.
N. M. R. in hydrate crystals: structural information from boradened fine-structure lines. (Journal of Chemical Physics, v. 38, Jan. 1, 1963, p. 61-69.)

Reich, H. A.
Nuclear magnetic resonance in solid helium-3. (Physical Review, v. 129, Jan. 15, 1963, p. 630-643.)

Suga, H. and Seki, S.
Availability of high-resolution n-m-r method for the study of molecular motion in the crystalline state. (Journal of Physics and Chemistry of Solids, v. 24, Feb. 1963, p. 330-331.)

1962

Anderson, W. A.
Applications of modulation techniques to high resolution nuclear magnetic resonance spectrometers. (Review of Scientific Instruments v. 33, Nov. 1962, p. 1160-1162.)

Anderson, A. G. and Hartman, S. R.
Nuclear magnetic resonance in the demagnetized state. (Physical Review, v. 128, Dec. 1, 1962, p. 2023-2041.)

Barnes, R. G. and Segel, S. L.
Nuclear magnetic resonance of Cl^{35} in paramagnetic $FeCl_2$. (Journal of Chemical Physics, v. 37, Oct. 15, 1962, p. 1895-1896.)

Butterworth, J.
Nuclear magnetic relaxation and shift in platinum. (Physical Review Letters, v. 8, June 1, 1962, p. 432-434.)

Motorola Systems Research Laboratory, Dodd, E. E.
Nuclear Magnetic Resonance Rate Gyro Performance, Technical Report No. RL-TR-3846-4 (April 1962.)

Dohnanyi, J. S.
Nuclear magnetic relaxation in the presence of paramagnetic ions. (Physical Review, v. 125, March 15, 1962, p. 1824-1831.)

Faulkner, E. A. and Ham, R. K.
Nuclear magnetic resonance, stored energy and the density of dislocations in deformed aluminum. (Philosophical Magazine, v. 7, Series 8, Feb. 1962, p. 279-284.)

Foster, H.
Magnetic resonance spectrometry. (Analytical Chemistry, v. 34, April 1962, p. 255R-261R.)
Survey of literature containing 155 references.

Gendell, J., Cotts, R. M. and Sienko, M. J.
Magnetic-resonance studies of lithium vanadium bronze. (Journal of Chemical Physics, v. 37, July 15, 1962, p. 220-225.)

Gossard, A. C. and Jaccarino, V.
Boron nuclear magnetic resonance in rare earth intermetallic compounds. (Physical Society Proceedings, v. 80, pt. 4, Oct. 1962, p. 877-881.)

Gossard, A. C., Jaccarino, V., and Wernick, J. H.
Nuclear magnetic resonance in UAl_2. (Physical Review, v. 128, Nov. 1, 1962, p. 138-143.)

Heller, P. and Benedek, G. B.
Nuclear magnetic resonance in MnF_2 near the critical point. (Physical Review Letters, v. 8, June 1, 1962, p. 428-432.)

Jones, W. H., Jr., Garbaty, E. A. and Barnes, R. G.
Nuclear magnetic resonance in metal tungsten bronzes. (Journal of Chemical Physics, v. 36, Jan. 15, 1962, p. 494-495.)

Mahendroo, P. P. and Nolle, A. W.
Nuclear Magnetic Relaxation in Ionic Crystals at High Temperatures, Phys. Rev., Vol. 126, no. 1, 125-129, (April 1, 1962).

McDonald, M. P. and Ward, I, M.
A nuclear magnetic resonance investigation of polypropylene. (Physical Society. Proceedings, v. 80, pt. 6, Dec. 1962, p. 1249-1263.)

Narath, A. and Wallace, D. C.
Nuclear magnetic resonance in cubic sodium tungsten bronzes. (Physical Review, v. 127, Aug. 1, 1962, p. 724-729.)

O'Reilly, D. E. and Tsang, T.
Analysis of nuclear magnetic resonance line shapes by lattice harmonics. (Physical Review, v. 128, Dec. 15, 1962, p. 2639-2654.)

Paul, D. I.
Nuclear magnetic resonance within an antiferromagnetic Bloch wall. (Physical Review, v. 127, July 15, 1962, p. 455-460.)

Pennington, K. S. and Petch, H. E.
Nuclear magnetic resonance spectrum of B^{11} in lesserite. (Journal of Chemical Physics, v. 36, April 15, 1962, p. 2151-2155.)

Reddoch, A. H. and Ritter, G. J.
Nuclear magnetic resonance of Lu^{175}. (Physical Review, v. 126, May 15, 1962, p. 1493-1495.)

Resing, H. A.
N. M. R. relaxation times in solid white phosphorus diffusion and rotation. (Journal of Chemical Physics, v. 37, Dec. 1, 1962, p. 2575-2583.)

Sagalyn, P. L. and Hofmann, J. A.
Nuclear magnetic resonance in metallic single crystals. (Physical Review, v. 127, July 1, 1962, p. 68-71.)

Schmugge, T. J. and Jeffries, C. D.
Sizeable Dynamic Proton Polarizations, Phys. Rev. Letters, Vol, 9, no. 6 (Sept. 15, 1962).

Shulman, R. G. and Wyluda, B. J.
Nuclear magnetic resonance shifts in rare earth nitrides. (Journal of Physics and Chemistry of Solids, v. 23, Jan.-Feb. 1962, p. 166.)

Solomon, I. and Ezratty, J.
Magnetic resonance with strong radio-frequency field in solids. (Physical Review, v. 127, July 1962, p. 78-87.)

Streever, R. L. and others
Nuclear magnetic resonances of Ni^{61} in dilute alloys of nickel in cobalt. (Physical Review, v. 128, Nov. 15, 1962, p. 1632-1633.)

Titman, J. M.
Nuclear magnetic resonance in Al-Ag alloys. (Journal of Physics on Chemistry of Solids, v. 23, March 1962, p. 318-320.)

Torgeson, D. R. and Barnes, R. G.
Nuclear magnetic resonance and Knight shift in solid indium. (Physical Review Letters, v. 9, Sept. 15, 1962, p. 255-257.)

Van Ostenburg, D. O., Trapp, H. and Lam, D. J.
Nuclear magnetic resonance of Tc^{99} in Tc metal and Tc^{99} and V^{51} in Tc-V alloys. (Physical Reviews, v. 126, May 1, 1962, p. 938-940.)

Walsted, R. E. and others
Nuclear magnetic resonance in platinum. (Physical Review Letters, v. 8, May 15, 1962, p. 406-408.)

Webb, W. E. and Moulton, W. G.
N. M. R. of a glycine single crystal. (Journal of Chemical Physics, v. 36, April 1, 1962, p. 1911-1913.)

Zupancic, I.
Current shims for high-resolution nuclear magnetic resonance on problem of correcting magnetic field inhomgeneities. (Journal of Scientific Instruments, v. 39, Dec. 1962, p. 621-624.)

1961

Androes, G. M. and Knight, W. D.
Nuclear magnetic resonance in super-conducting tin. (Physical Review, v. 121, Feb. 1, 1961, p. 779-787.)

Benedek, G. B. and Armstrong, J.
Pressure and temperature dependence of frequence of the Fe^{57} nuclear magnetic resonance frequency in ferromagnetic iron. (Journal of Applied Physics, v. 32, Supllement, March 1961, p. 106s-110s.)

Bonera, G. and DeStefano, P.
Transient effects in nuclear magnetic resonance with the rotating co-ordinates method. (Nuovo Cimento, v. 20, April 16, 1961, p. 316-323.) In English.

Bray, P. J. and others
Nuclear magnetic resonance studies of B^{11}. (Journal of Chemical Physics, v. 35, Aug. 1961, p. 435-452.)

Bruner, L. J., Budnick, J. I. and Blume, R. J.
Nuclear magnetic resonance of Ni^{61} in metallic nickel. (Physical Review, v. 121, Jan. 1, 1961, p. 83.)

Budnick, J. I. and others
Nuclear magnetic resonance of Fe^{57} in unenriched Fe. (Journal of Applied Physics, v. 32, Supplement, March 1961, p. 120s-121s.)

Burns, G.
Nuclear magnetic resonance in $(NH_4)_2$ $(BeF_4)x(SO_4)$ 1-x and other ferroelectric systems. (Physical Review v. 123, July 1, 1961, p. 64-66.)

Cowan, J. A. and Kaplan, D. E.
Spin-Echo Measurement of the Spin-Lattice and Spin-Spin Relaxation in Ce^{3+} in Lanthanum Magnesium Nitrate, Phys. Rev. Vol. 124, no. 4., 1098 (1961).

Flynn, C. P. and Seymour, E. F. W.
Diffusion narrowing of nuclear magnetic resonance in aluminm and copper. (Physical Society Proceedings, v. 77, Pt. 4, April 1961, p. 922-930.)

Ghosh, S. K. Lahiri, J. and Sinha, SK.
F^{19} nuclear magnetic resonances in polycrystalline MgF_2. (Indian Journal of Physics, v. 35, May 1961, p. 236-239)

Goldburg, W. I.
Nuclear magnetic resonance saturation in NaCl and CaFe. (Physical Review, v. 122, May 1, 1961, p. 831-833.)

Gossard, A. C., Portis, A. M. and Sandle, V. W. G.
Nuclear magnetic resonance in ferromagnetic Fe. (Journal of Physics and Chemistry of Solids, v. 17, Jan. 1961, p. 341-342.)

Hardy, W. A.
Nuclear resonance in cubic, hexagonal and mixed phase cobalt powders and thin films. (Journal of Applied Physics, v. 32, Supplement, March 1961, p. 122s-123s.)

Jaccarino, V.
N. M. R. and the conduction of electron polarization in rare earth metals. (Journal of Applied Physics, v. 32, Supplement, March 1961, p. 102s-106s.)

Leifson, O. S. and Jeffries, C. D.
Dynamic Polarization of Nuclei by Electron - Nuclear Dipolar Coupling in Crystals, Phys. Rev. Vol 122, no. 6, 1781 (1961).

Milford, F. J. and Gager, W. B.
Knight shift in potassium. (Physical Review, v. 121, Feb. 1, 1961, p. 716-720.)

Narath, A.
Nuclear magnetic resonance of Cr^{53} in antiferromagnetic $CrCl_3$. (Physical Review Letters, v. 7, Dec. 1, 1961, p. 410-411.)

Ragle, J. L.
Anisotropy of nuclear magnetic resonance in vanadium pentoxide. (Journal of Chemical Physics, v. 35, Aug. 1961, p. 753-754.)

Shulman, R. G.
Nuclear magnetic resonance and magnetic ordering in NiF_2. (Physical Review, v. 121, Jan. 1, 1961, p. 125-143.)

Shulman, R. G.
Nuclear magnetic resonance in NiF_2 domain walls. (Journal of Applied Physics, v. 32, Supplement, March 1961, p. 126s-128s.)

Shulman, R. G. and Wyluda, B. J.
Nuclear magnetic resonance in $CuF_2 \cdot 2H_2O$ single crystals. (Journal of Chemical Physics, v. 35, Oct. 1961, p. 1498-1499.)

Slichter, C. P.
Nuclear magnetic resonance studies of elastomers. (Rubber Chemistry and Technology, v. 34, Dec. 1961, p. 1574-1600.)

Street, R., Rodbell, D. S. and Roth, W. L.
Nuclear magnetic resonance spectrum of Co^{59} in metallic cobalt powders. (Physical Review, v. 121, Jan. 1, 1961, p. 84-86.)

Van der Lugt, W. and Poulis, N. J.
The splitting of the nuclear magnetic resonance lines in vivianite. (Physica, v. 27, Aug. 1961, p. 733-750.)

Woessner, D. E.
Effects of diffusion in nuclear magnetic resonance spin-echo effects. (Journal of Chemical Physics, v. 34, June 1961, p. 2057-2061.)

1960

Andrew, E. R. and others
Fine structure of the nuclear magnetic resonance spectra of solids: chemical shift structure of the spectrum of phosphorus pentachloride. (Nature, v. 188, Dec. 24, 1960, p. 1096-1097.)

Benedek, G. B. and Kushida, T.
Nuclear magnetic resonance in antiferromagnetic MnF_2 under hydrostatic pressure. (Physical Review, v. 118, April 1, 1960, p. 46-57.)

Blumberg, W. E., and others
Correlations between super conductivity and nuclear magnetic resonance properties. (Physical Review Letters, v. 5, Aug. 15, 1960, p. 149-152.

Budnick, J. I.
Nuclear magnetic resonance in tantalum. (Journal of Physics and Chemistry of Solids, v. 16, Nov. 1960, p. 37-38.)

Cornell University
Solid State Physics, Lithium, Ions, Diffusion, Lithium Compounds, Vanadium Lattices, Nuclear Magnetic Resonance, Electrons, Spin-Relaxation time, Paramagnetic Resonance, Nuclear Spins. Ithaca, N. Y. Astia Document AD - 275 086 62-3-3 Div. 25.

Faulkner, E. A.
Strain-broadening of nuclear magnetic resonance lines in copper. (Philosophical Magazine, v. 5, Series 8, Aug. 1960, p. 843-851.)

Freeman, R. and Pound, R. V.
High resolution N. M. R. spectrometer with the radio frequency controlled by the magnetic field. (Review of Scientific Instruments, v. 31, Fab. 1960, p. 103-106.)

Frey, D. A. and Weaver, H. E.
N. M. R. measurements of the Knight shift in conducting PbO_2. (Electrochemical Society Journal, v. 107, Nov. 1960, p. 930-932.)

Holuj, F. and Petch, H. E.
A nuclear magnetic resonance study of colemanite. (Canadian Journal of Physics, v. 38, April 1960, p. 515-546.)

Hyde, J. S.
Magnetic Resonance and Rapid Passage in Irradiated Li F, (Phys. Rev. Vol. 119, no. 5, 1483, 1960.)

Hyndman, D. and Origlio, G. F., NMR Absorption in Teflon Fibers, JAP, Vol. 31, 1849 (1960).

Ibers, J. A.
Nuclear magnetic resonance study of polycrystalline NH_4CO_4. (Journal of Chemical Physics, v. 32, May 1960, p. 1448-1449.)

Klein, M. P. and Knight, W. D.
Nuclear magnetic resonance in metallic potassium. (Journal of Physics and Chemistry of Solids, v. 15, Oct. 1960, p. 355-356.)

Portis, A. M. and Gossard, A. C.
Nuclear Resonance in Ferromagnetic Cobalt, JAP supplement, Vol. 31, 205s (1960).

Motorola Systems Research Laboratory, Pake, G. E.
Nuclear Magnetic Relaxation Times, Technical Report No. RL-TR-3846-1, Astia Document AD 242654 (August 1960).

Pennington, K. S. and Petch, H. E.
Nuclear magnetic resonance spectrum of B^{11} in inderite. (Journal of Chemical Physics, v. 33, Aug. 1960, p329-334.)

Pound, R. V. and Freeman, R.
Frequency control of an oscillator by nuclear magnetic resonance. (Review of Scientific Instruments, v. 31, Feb. 1960, p. 96-102.)

Rogers, M. T.
Some chemical applications of nuclear magnetic resonance. (Record of Chemical Progress, v. 21, Dec. 1960, p. 197-210.)

Rowland, T. J.
Nuclear magnetic resonance in copper alloys. Electron distribution around solute atoms. (Physical Review, v. 119, Aug. 1, 1960, p. 900-912.)

Shulman, R. G. and Knox, K.
Nuclear magnetic resonance in $KMnF_3$. (Physical Review, v. 119, July 1, 1960, p. 94-101.)

Silver, A. H. and Bray, P. J.
N. M. R. study of bonding in some solid boron compounds. (Journal of Chemical Physics, v. 32, Jan. 1960, p. 288-292.)

Stout, J. W. and Shulman, R. G.
Nuclear magnetic resonance in paramagnetic FeF_2. (Physical Review, v. 118, June 1, 1960, p. 1136-1141.)

Turner, J. J.
Use of complex wiggle-beat patterns for the estimation of small splittings in NMR spectra. (Molecular Physics, v. 3, Sept. 1960, p. 417-424.)

Walter, G. K.
Application of magnetic resonance techniques to the study of semiconductor surfaces. (Journal of Physics and Chemistry of Solids, v. 14, 1960, p. 43-50.)

Washington University
Nuclear Magnetic Resonance in Spinning Solids and Metals, Astia Document AD 2822396.

Weinberg, D. L.
Nuclear magnetic resonance intensities in alloys. (Journal of Physics and Chemistry of Solids, V. 15, Oct. 1960, p. 249-260.)

General Electric Research Laboratory; Webb, M. B.
Nuclear Magnetic Resonance Study of Metals and Alloys. Astia Document AD 247407 (October 1960).

U. S. N. Postgraduate School, Twining, D. S.
A Feasibility Study of an Atomic Rate Gyro, Master of Science Thesis (1960).

M. I. T., Neufeld, M. J.
Nuclear Magnetism as Space Reference, Master of Science Thesis, Department of Aeronautical Engineering, Report T-82, May 1955, Astia Document AD 121874).

1959

Andrew, E. R.
Nuclear magnetic resonance in solids. (British Journal of Applied Physics, v. 10, Oct. 1959, p. 431-437.)

Bolef, D. I. and Menes, M.
Nuclear magnetic resonance acoustic absorption in Kl and KBr. (Physical Review, v. 114, June 15, 1959, p. 1441-1451.)

Bonera, G. and Giulotto, L.
Adiabatic passages in nuclear magnetic resonance with the rotating co-ordinate method. (Nuovo Cimento, v. 14, Oct. 16, 1959, p. 435-442.) In English.

Brownstein, S.
High-resolution nuclear magnetic resonance and molecular structure. (Chemical Reviews, v. 59, 1959, p. 463-496.)

Brownstein, S.
A simple thermostated probe assembly for high resolution nuclear magnetic resonance spectra. (Canadian Journal of Physics, v. 37, June 1959, p. 1119-1121.)

Chidambaram, R.
A method of reducing radiation damping in nuclear magnetic resonance. (Nuovo Cimento, v. 13, July 16, 1959, p. 405-409.) In English.

Dessy, R. E. and others
Nuclear magnetic resonance spectra of some dialkylmercury compounds. (Journal of Chemical Physics, v. 30, June 1959, p. 1422-1425.)

Dharmatti, S. S., Sundara, Rao K. J. and ViJayaraghavan, R.
The construction and working of a wide line nuclear magnetic resonance spectrometer and the measurements of some chemical shifts. (Nuovo Cimento, v. 11, March 1, 1959, p. 656-669.) In English.

Drain, L. E.
Nuclear magnetic resonance in silver-cadmium. (Philosophical Magazine, v. 4, Series 8, April 1959, p. 484-501.)

Holm, C. H. and Ibers, J. A.
NMR study of ferrocene, ruthenocene and titanocene dichloride. (Journal of Chemical Physics, v. 30, April 1959, p. 885-888.)

Hon, J. F. and Bray, P. J.
Nuclear magnetic resonance studies of neutron irradiated alkali halides. (Journal of Physics and Chemistry of Solids, v. 11, Sept. 1959, p. 149-169.)

Kapur, K. N. and McGrath, J. W.
Wide r. f. unit for an N. M. R. spectrometer. (Review of Scientific Instruments, v. 30, April 1959, p. 272-274.)

McCall, D. W. and Hamming, R. W.
Nuclear magnetic resonance in crystals. (Acta Crystallographica, v. 12, Feb. 1959, p. 81-86.)

McGarvey, B. R. and Slomp, G., Jr.
N. M. R. spectrum of the ethyl group. An exact solution. (Journal of Chemical Physics, v. 30, June 1969, p. 1586-1589.)

Oliver, D. J.
Nuclear magnetic resonance in gallium antimonide. (Journal of Physics and Chemistry of Solids, v. 11, Oct. 1959, p. 257-262.)

Piette, L. H. and Anderson, W. A.
Potential energy barrier determinations for some alkyl nitrates by nuclear magnetic resonance. (Journal of Chemical Physics, v. 30, April 1959, p. 899-908.)

Rocard, J. M. Bloom, M. and Robinson, L. B.
Nuclear magnetic resonance in lead-containing compounds. (Canadian Journal of Physics, v. 37, April 1959, p. 522-525.)

Silver, A. H. and Bray, P. J.
Nuclear magnetic resonance study of boron carbide. (Journal of Chemical Physics, v. 31, July 1959, p. 247-253.)

Ward, I, M.
Nuclear magnetic relaxation in polyethylene deuteroterephtalate. (Journal of Chemical Physics, v. 31, Sept. 1959, p. 858-859.)

West, G. W.
Nuclear magnetic resonance in physical metallurgy. (Australian Institute of Metals. Journal v. 4, Nov. 1959, p. 156-163.)

Selected references prior to 1950.

Bloch, F. - "Nuclear Induction," Phys. Rev. 70, 460 (1946).

Van Vleck, J. H., Dipolar Broadening of Magnetic Resonance Lines in Crystals, Phys. Rev., Vol. 74, no. 9, 1168-1183 (1948).

Pound, R. V., Nuclear Electric Quadrupole Interactions in Crystals, Phys. Rev., Vol. 79, no. 4, 685-702 (1950).

Pound, R. V., Nuclear Spin Relaxation Times in Single Crystals of LiF, Phys. Rev., Vol 81, no. 1, 156 (1951).

Purcell, E, M. and Pound, R. V., Nuclear Spin System at Negative Temperature, Phys. Rev., Vol. 81, no. 2, 279 (1951).

Redfield, A. G., Nuclear Magnetic Resonance Saturation and Rotary Saturation in Solids, Phys. Rev., Vol. 98, no. 6, 1787 (1955).

Jaccarino, V. and Shulman, R. G., Observation of Nuclear Magnetic Resonance in Antiferromagnetic Mn (F^{19})2, Phys. Rev., Vol. 107, 1196 (1957).

Whitfield, G. and Redfield, A. G., Paramagnetic Resonance Detection Along the Polarizing Field Direction, Phys. Rev., Vol 106, no. 5 (June 1, 1957).

Abragam, A., Proctor, W. G., Spin Temperature, Phys. Rev. Vol 109, no. 5, 1441 (1958).

APPENDIX II

Dynamic Nuclear Polarization by Microwave Pumping in Solids; Enhancement of Nuclear Resonance Signals

BY PROF. C. D. JEFFRIES

A. Principle of Method

The method which is applicable to solids containing a large fraction of the nuclei of interest is the method of saturation of forbidden transitions in electron-nuclear dipolar coupling. We have developed this method here to such an extent that we obtain approximately 70% (corresponds to increase of 2×10^5 of M_o) proton polarizations for all the protons in $(Nd, Ca)_2 Mg_3 (NO_3)_{12} \quad 24H_2O$. This method is called the "effect solids" by the Saclay group. Basic references are:

1. C. D. Jeffries, Phys. Rev. 117, 1056 (1960), Part III.
2. O. S. Leifson and C. D. Jeffries, Phys. Rev. 122, 1781 (1961).
3. T. J. Schmugge and C. D. Jeffries; Phys. Rev. Letters 9, 268 (1961).
4. Dynamic Nuclear Orientation, C. D. Jeffries, John Wiley (1963, in press).

A representative sample for which this method works is a single crystal (say a flat hexagonal plate 1 cm in diameter X 2 mm thick) of $(N_{d}^{1:99}, L_a)_2 Mg_3 (NO_3)_{12} \cdot 24H_2O$. The paramagnetic Nd^{3+} ions form an $S = \frac{1}{2}$ electron spin system; the protons in the waters of hydration form an $I = \frac{1}{2}$ nuclear spin system. Place the crystal in a magnetic field H_o; the energy levels will be labeled by $\langle S_z \rangle = M_s = \pm \frac{1}{2}$, and $I_z = M_z = \pm \frac{1}{2}$

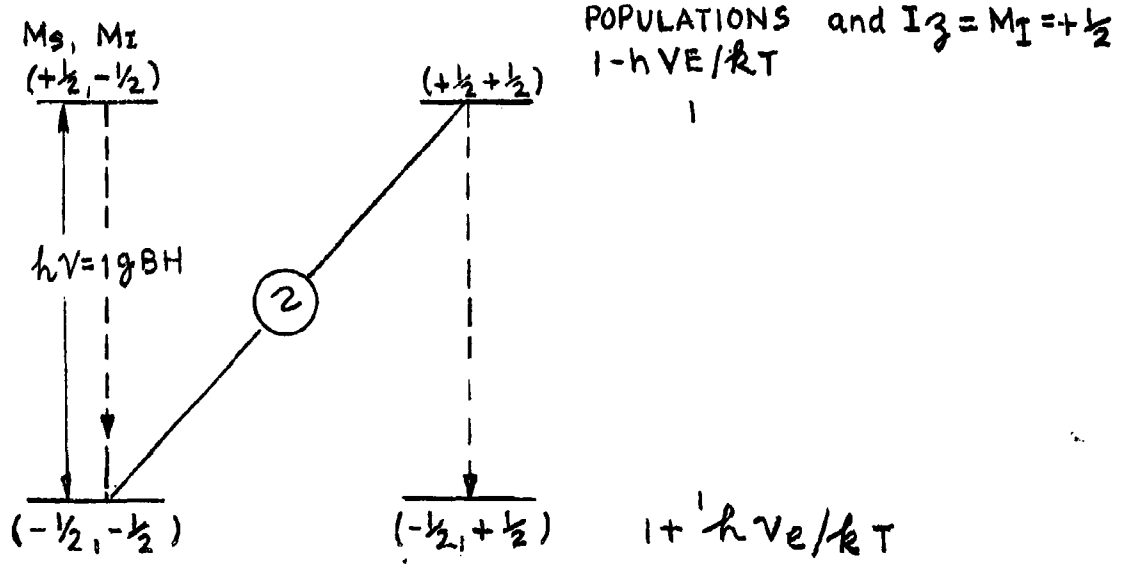

The crystal must be irradiated with a H_1 field at the microwave frequency $\nu = \nu_e - \nu_n$ as shown. This will saturate the so-called forbidden transitions $(+\frac{1}{2}, +\frac{1}{2}) \longleftrightarrow (-\frac{1}{2}, -\frac{1}{2})$ corresponding to flipping both electrons and nuclear spins. The relative populations of the levels become as shown, if we also include the effect of the dominant electron spin-lattice relaxation, shown as $\overline{\underline{I}}$ $\underline{\overline{I}}$ The nuclear polarization is thus

$$P_{nuc} \equiv \frac{N\,(M_I = +\frac{1}{2}) - N\,(M_I = -\frac{1}{2})}{N\,(M_I = +\frac{1}{2}) + N\,(M_I = -\frac{1}{2})}$$

$$\equiv h\nu_{e/2KT} \sim 1 \quad \left\{ \text{at } \begin{array}{l} \nu_e \sim 10^{10} \\ T \sim 1^\circ K \end{array} \right.$$

To reduce this to the nuclear magnetization, we write the enhanced magnetization as $M_{enh} = M_o \times \frac{\nu_e}{\nu_n} \approx M_o \times 500$, typically. Thus this method gives an enhancement of the magnetization (and hence of the nuclear reso-

nance signal) by a factor around 500. Experiments here have verified this enhancement for this crystal, under the conditions:

$T = 1.5°K$ $\qquad T_1 = 10^3$ sec

$V_e = 75$ KM$_c$ $\qquad T_2 = 10^{-5}$ sec

$H_o \approx 20$ koe

crystal mass $\approx$ 100 milligrams up to 20 grams.

When the nuclear magnetization is as large as this (10^5 X longer than usual) we find that the detector coil Q is visibly lowered by the resonance; it is that strong.

If the frequency $V = V_e + V_n$ is used instead of $V = V_e - V_n$ the magnetization is similarly enhanced, but reversed in sign. This increases the coil Q, and it is possible to obtain maser action, i.e. the coil Q is effectively increased to infinity and the system becomes an auto-oscillator at the nuclear frequency V_n.

To summarize, by dynamic proton polarization in solids at helium temperatures, it is possible to obtain an increase of M_o by $\approx 10^5$ over its room temperature thermal-equilibrium value. This would correspondingly increase the signal voltage V^1_y by the same factor, where V^1_y is the initial free precession signal voltage after a 90° pulse.

This method can also be made to work for say $(CH_2)_n$ (irradiated with γ - rays to produce unpaired electron spins) at room temperature or liquid N_2 temperature. Generally speaking the enhancements observed are not as large as for helium temperatures, but lie in the range 10X to 100X.

B. Applications to Nuclear Gyros

If the pulse-precession method is used for sampling the nuclear magnetization, it would appear that a larger S/N ratio would be obtainable in solids at low temperatures, particularly if the polarization is dynamically enhanced. However if CW methods are used, where $V_{\text{signal}} \propto \sqrt{\frac{T_2}{T_1}}$ probably not much will be gained by using solids at low temperatures.

The apparatus necessary to obtain an enhancement of 500X at helium temperatures is not simple nor widely known. In the first demonstrations we have used large (2 to 10 ton) electro magnets, complex microwave equipment (e.g. klystrons of several watts power at 4 to 8 mm wave length), complex helium dewars, etc. All of this is far more complex and bulky than the room temperature apparatus, and its application to nuclear gyros is not easy, if the weight of the equipment is a consideration.

However if weight is not a factor and pulse-precession methods are used, (where signal $\propto$ M) then far longer signal to noise ratios will be obtained in solids at low temperatures.

C. Possible Reduction in Line Width in Solids at Low Temperatures

For really high dynamic nuclear polarizations ($\approx$ 90%) the nuclear resonance line width in solids should become considerably narrower.

5. Reference: K. Kawke and T. Usui, Progr. Theor. Phys. (Kyoto) 8, 302 (1952).

Generally speaking, the result of ref. 5 is that

$$\langle \Delta H \rangle^2 \approx \langle \Delta H^2 \rangle_0 \left[1 - \left(\frac{h V n}{2 k T} \right)^2 + - - - \quad 1 \right.$$

where $\sqrt{\langle \Delta H \rangle_0^2}$ is the usual Van Vlecks line width observed, and also calculated for $h V n / kT \ll 1$. Here however we should use for T the effective nuclear spin temperature. For very high polarizations, $hV/2KT \approx 1$ so that the line width should narrow, or even split up into several lines, (each very sharp), if there are unequivalent lattice sites for the nuclei. The reason the line narrows is that for complete alignment all the local fields throughout the crystal are completely determined exactly. There is no possibility that a neighbor nucleus may be either up or down, thus smearing out the local field.

We have observed recently the beginning of this narrowing, roughly, by only a factor 2, at a polarization of 70%. However, there is this interesting theoretical possibility that one could get very narrow lines and high magnetization M_0 simultaneously in solids at very low temperatures, obtained dynamically. More basic work needs to be done before it may be realized and this is fairly speculative.

APPENDIX III

Problem of Magnetic Dilution of Nuclear Spins: Does this give an increased signal/noise ratio?

BY PROF. C. D. JEFFRIES

A. References:

1. Abragam, pp. 125-127.
2. Kittel and Abrahams, Phys. Rev. 90, 238 (1953).

The theoretical predictions (not yet experimentally verified) are that upon dilution a line will be narrowed: a) with a line width proportional to the square root of the concentration for dilutions $> \frac{1}{10}$; and b) with a line width proportional to the concentrations for dilutions $< \frac{1}{100}$. We examine this effect on the signal, Part II for both CW and pulse detections schemes.

B. CW Detection

Part II, eq. (5), signal voltage is proportional to $V_y \propto N \sqrt{T_2}$. In case a) above let $N = N_o f$, where N_o is the undiluted nuclear spin concentration and is the fractional concentration used in the dilution. Then, since

$$\Delta H = (\Delta H)_o \sqrt{f} \propto \frac{1}{T_2}, \qquad V_y \propto (N_o f) \times \frac{\sqrt{T_{20}}}{\sqrt{f}} = N_o T_{20} \cdot f^{3/4}$$

Thus decreasing the concentration only reduces the signal; $f > 0.1$

In case b) $N = N_o f \qquad f < .01$

$$T_2 = T_{20/f}$$

$$V_y \propto (N_o f) \sqrt{\frac{T_{20}}{f}} = N_o T_{20} f^{1/2}$$

The signal is reduced by reducing the concentration.

C. Pulse Detection

Part II, eq. (7), signal is proportional to $V_y^1 \quad N_e^{-t/T_2}$

case a) $V_y^1 \propto N_o f e^{-t\sqrt{f}/T_{20}}$ $\quad f > .1$

case b) $V_y^1 \propto N_o f e^{-tf/T_{20}}$ $\quad f < .01$

In either case the signal is reduced upon dilution, but it decays at a less rapid rate. It is difficult to say if a net advantage is gained in overall S/N unless more is specified about the details of the detection scheme, the duty cycles involved, etc.

Generally, however, it appears that magnetic dilution can only reduce the signal/noise ratio.

APPENDIX IV

Possibility of Obtaining Enhanced Nuclear Polarization by Optical Pumping Methods

BY PROF. C. D. JEFFRIES

A. Gases

Almost all the work has been done on gases, so we mention this as background for speculation on solids.

a) Optical pumping polarization of

1. Reference: Shearer, Colegrove and Walters, Phys. Rev. Letters 10, 108 (1963), and earlier references No. 1 and No. 2 given in this paper.

This method is experimentally very simple: one simply shines a special lamp onto a bulb of H_e^3 gas at about 1 mm. pressure. A large enhancement of the nuclear polarization is produced by exchange-of-metastability collision of H_e^3 atoms with excited H_e^3 atoms. Polarization of up to 60% (private communication) have been obtained. However, the nuclear spin density is 10^5 lower than matter of normal density so that this doesn't really give large signals. The relaxation time is rather long: $T_1 \approx 600$ seconds and T_2 is entirely determined by field in homogeneity.

b) A variety of other slightly different optical pumping methods for gases exist and do work. However, all operate at similar pressures (1 mm) and so nuclear resonance signals would be small, even though a larger enhancement is obtained. For a review article, see F. Bitter, Applied Optics, Vol. 1, page 1 (1962).

B. Speculations on Solids

We review an example from gases, as indicative of the method. (Reference: F. Bitter, et al, Rev. Mod Phys. 25, 174, 1953; this paper gives the theory; the method has now been made to work.)

Consider a gas of H_g^{199} vapor, for which the nuclear spin is $I = \frac{1}{2}$. The ground state of H_g atoms is $^1S_0$; the excited state is $^3P_1$.

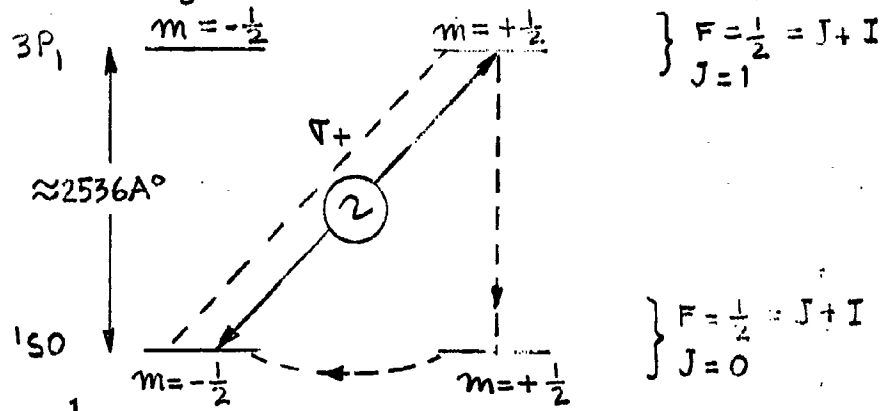

Only the $F = \frac{1}{2}$ levels of the excited state are shown. If the vapor is illuminated with circularly polarized light (σ_+), only the transitions $(^1S_0, m = -\frac{1}{2}) \longrightarrow (^3P_1, m = +\frac{1}{2})$ will be induced upward, as shown.

APPENDIX V

Ultimate Limitations of Nuclear-Gyro Precision

BY PROF. C. D. JEFFRIES

A. Problem

The aim of the gyro is to measure the orientation of a direction $\hat{\ell}$ fixed in absolute space and defined by an initial nuclear magnetization $\vec{M} = M_o \hat{\ell} = M_o \hat{z}$ relative to vehicle axes x, y, z.

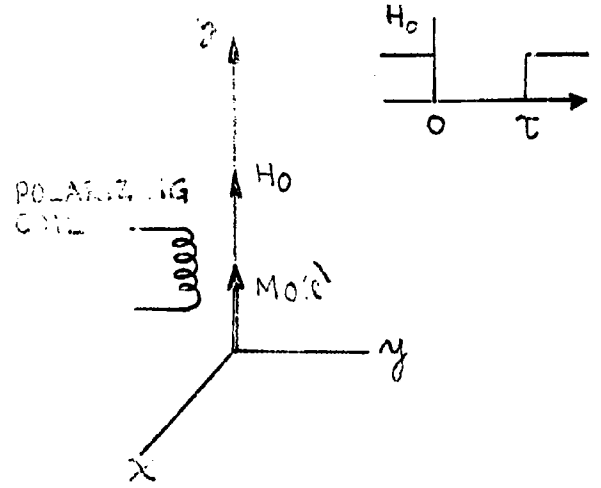

Initial orientation, just prior to non-adiabatic cut-off of H_o

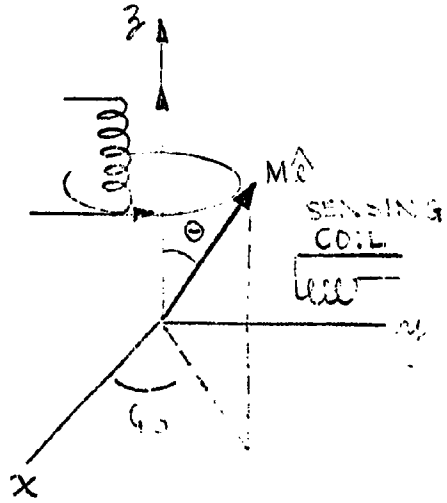

Orientation a time τ later, at instant H_o is reapplied

During the time $0 \leq \tau \leq t$, $M\hat{\ell}$ is reoriented to the position given by (Θ, ϕ_o) due to the motion of the x, y, z axes.

When H_o is reapplied $M\hat{\ell}$ precesses about z, and will induce a voltage V_y in the sensing coil given by

$$V_y = \frac{d\tilde{\phi}}{dt} = A \frac{dB_y}{dt} = A \frac{d}{dt}(\bar{H}_y + 4\pi M_y)$$

$$M_y = M \sin\Theta \sin\phi \qquad \phi = \phi_o + w(t - \tau)$$

$$V_y = M \sin\Theta \sin\left[\phi_o + w(t - \tau)\right]$$

The magnitude V_y determines the angle Θ.

The phase of V_y at $t = \tau$ determines the angle φ_o.

The angles Θ, φ_o are to be measured, or rather, a servo is to reorient the x, y, z axes so that $\Theta \to 0$, $\varphi_o \to 0$. That is, we now let x, y, z be the axes of a platform in the vehicle which is to be constantly realigned so that $z \parallel \hat{\mathcal{H}}$. Actually we see that since $|V_y| \propto M \sin \Theta$ there will be an uncertainty in Θ if there is an uncertainty in M, or rather a fluctuation in M. We estimate that fluctuations in M for several processes below. M is the magnetic dipole moment per unit volume.

B. Fluctuation in M due to random relaxation

If M is the magnetization at time t = o, then at later times, $M = M_o e^{-t/T_1}$ where T_1 is the nuclear spin - lattice relaxation time. This equation is similar in form and interpretation to the radioactive decay equation: $C = C_o e^{-t/T_1}$.

In a time dt there will be dC decays,

$$dC = C_o e^{-t/T_1} \left(\frac{1}{T_1}\right) dt$$

$$dC \approx \frac{C_o}{T_1} dt_1 \quad \text{if } t \ll T_1$$

Because of the random nature of the decay, there will be a statistical fluctuation Δ (dC) in the number of counts, given by

$$\Delta (dc) \approx \sqrt{dc}$$

We can think of the polarized nuclear spin system as made up of $N_o = N \frac{\mu H_o}{2kT}$ effective number of spins pointing up initially, where N is the number of protons. These relax at a rate $\frac{1}{T_1}$ per sec. by a random process, so that in a time interval τ the number to relax is

$$dn \cong \frac{\tau}{T_1} N_o$$

and the fluctuation in that number is

$$\Delta (dn) \approx \sqrt{\frac{\tau}{T_1} N_o}$$

This is also the fluctuation in the number remaining up. The total magnetization is just $M = \mu n = \mu N \frac{\mu H}{2kT}$ so that the fractional uncertainty in the total magnetization is just given by

$$\frac{\Delta M}{M} \approx \frac{n}{n_o} \sqrt{\frac{\tau}{T_1} N_o} \frac{1}{N_o} \approx \sqrt{\frac{\tau}{T_1} \frac{1}{n_o}}$$

Note that $n_o = N \left(\frac{\mu H_o}{2kT}\right)$ where μ = proton magnetic moment; H_o - polarizing field; T = spin temperature of protons = $\frac{T \text{ (lattice)}}{\text{enhancement}}$ N = total number of protons in sample.

This fluctuation $\frac{\Delta M}{M}$ is thus proportional to $\frac{1}{\sqrt{N}}$, as expected, and also proportional to $\sqrt{\tau}$, which is the kind of time dependence one finds in a random-walk diffusion problem. This process will give an uncertainty in angle of order $\Delta M/M$.

C. Fluctuation in direction of M due to local fields

Assume that a proton sees a local field $H_{LOC} \approx \mu/r^3$ from its nearest proton neighbor. $H_{LOC} \approx 2$ gauss, typically. Now in a short time τ_c the precession angle will be $\theta_L \approx W_{LOC} \tau_c = \gamma H_{LOC} \tau_c$.

The time τ_c is the Debye correlation time of the liquid and is the mean free time an individual proton precesses in a fixed local field before being interrupted by a molecular collision, which redirects the local field. We use the result of the random - walk problem to see that after n collisions the rms precession angle will be

$$\theta^2 = \tau_c \sqrt{N} \approx W_{LOC} \tau_c V_n$$

Now $n = \frac{\tau}{\tau_c}$ number of collisions in time τ, so that

$$\theta^2 \approx W_{LOC} \tau_c \sqrt{\frac{\tau}{\tau_c}} = W_{LOC} \sqrt{\tau \tau_c}$$

Noting that we have a total of N protons, each of which has a random direction of precession, the average spread of direction of magnetization for the whole sample will be

$$\epsilon = \left(\sqrt{\theta^2}\right)_{\substack{\text{sample}\\ \text{ave}}} \frac{2}{N} \frac{1}{\sqrt{N}} W_{L0C} \quad c$$

If we use $\frac{1}{T_2} \approx W_{L0C}^2 \cdot \tau_c$ for motionally - narrowed line, we get the result

$$\epsilon = \frac{1}{\sqrt{N}} \sqrt{\frac{2}{T_2}}$$

D. Estimate of component of M perpendicular to z due to fluctuations because of finite sample.

In the absence of an external magnetic field the megnetization of a collection of spins is zero about any direction, but the distribution is of interest. This may be calculated as in the random walk problem. From Kittel, Elementary Statistical Mechanics, P. 21-25, (John Wiley, 1958) and Kennard Kinetic Theory of Gases, P. 268-271, (Mc Graw Hill 1938) we see that about any direction, say the x direction, the total magnetization of the sample has one value $M_x = 0$ but $M_x^2 \sim N$, where μ is the proton moment and N is the total number of protons. Thus we reason as follows. We initially prepared the sample with a magnetization $M_z \sim \frac{H_0}{2kT} N$ in the z direction, by means of the polarizing field H_0. The field is cut off and we ask what is the rms magnetization in the x direction. The ratio

M_x^2/M_z will be an indication of the statistical angular spread due to finite sample number:

$$\frac{M_x^2}{M_z} \sim \frac{N}{\frac{H_0}{2kT} N} \sim \frac{1}{N} \frac{2kT}{H_0}$$

If the polarization is enhanced by the Overhouser effect, T becomes reduced by the enhancement ratio.

E. Evaluation

1. From II, $\frac{M}{M} \sim \frac{1}{T_1 n_0} \sim \frac{1}{T_1} \frac{1}{N} \frac{2kT}{H_0}$

Take $N \approx 10^{24}$ protons, $\tau \approx 0.1$ sec, T_1 1 sec

$$\frac{\Delta H_o}{2kT} \approx \frac{5 \times 10^{-24} \times 2.7 \times 300 \text{ gauss}}{2 \times 1.38 \times 10^{-16} \times 300^\circ \text{ K}} = 10^{-7}$$

$$\frac{\Delta M}{M} \approx 10^{-9}$$

2. From III,

$$\Delta\Theta \approx \frac{1}{\sqrt{N}} W_{LOC} \tau_c$$

$W_{LOC} \approx 10^5 \text{ sec}^{-1}$, $\tau = 0.1$

$\tau_c \approx 10^{-11}$ sec $\quad N = 10^{24}$

$\Delta\Theta \approx 10^{-13}$

3. From IV,

$$\Delta\Theta \approx \frac{1}{\sqrt{N}} \frac{2kT}{\mu H_o}$$

$N = 10^{24}$

$$\frac{H_o}{2kT} \approx 10^{-7}$$

$$\Delta\Theta \approx 10^{-5}$$

This is the longest effect. This will be reduced by factor 100 if Overhauser enhancement of 100 x is used.

F. Other effects

It seems to me that the largest uncertainties will come from practical considerations, i.e., instrumental effects. Suppose that the polarizing and/or precessing field has an inhomogeneity, $\Delta H/H$. This will give rise to a frequency spread $\Delta W/W \approx \Delta H/H$ and thus the voltage $V_y \propto WM \cos Wt$ will have a spread in frequencies which makes it difficult to measure exactly the magnitude and initial phase - these are needed to determine (see p. 93) Θ and Θ_c.